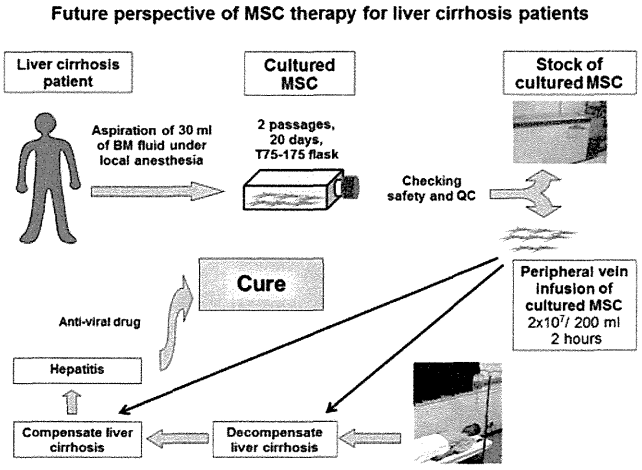

FIG. 3. Schematic representation of the therapeutic method of cultured MSC for liver cirrhosis patients.

with decompensated liver cirrhosis could be cultured and advanced into the mesenchymal stem cell stage, and then be administered through the peripheral vein. The results showed no adverse effects, and at 24 weeks, the model for end-stage liver disease score and liver volume showed improvements in two and three patients, respectively. An improvement in health-related Quality of Life parameters measured by the short form 36 [Medical Outcomes Study 36-Item Short-Form Health Survey (SF-36)] was also confirmed in this study.[17]

Status of the development of a liver-repair-and-regeneration therapy by using the next-generation BMCs

For the development of a minimally invasive treatment, we are conducting research and development investigations while taking into account the guidelines for clinical research on human stem cells.

Flow of the study

1. Establishment of proof-of-concept by using small animal models
2. Evaluation of safety and efficacy by using large- and middle-sized animal models
3. Preparation of clinical research
4. Evaluation of the safety of cultured cells by using cell processing centers (isolators)
5. Clinical research (application for human stem cells).

Establishment of proof-of-concept using small animal models. Our previous treatment regimen based on the administration of autologous BMCs should activate hepatic progenitor cells, induce the proliferation of hepatocytes, and improve the fibrosis associated with liver cirrhosis. In this case, BMCs were introduced through the peripheral blood vessels. We also assessed whether BMCs improved the symptoms of liver fibrosis. To achieve this, we purchased commercially available human bone marrow-derived mononuclear cells (Lonza, Inc., Basel, Switzerland) and evaluated their capability to improve fibrosis in the CCl_4-induced cirrhosis model in SCID mice.[18] Stable cultures of mesenchymal cells were indeed obtained, and our assessments validated that they could improve fibrosis.

Evaluation of safety and efficacy by using large- and middle-sized animal models. In our treatment strategy, we cultured mesenchymal cells from autologous bone marrow aspirated from beagle dogs. These cells were then administered to the same dogs through peripheral blood vessels in approximately three times the quantities delivered by other methods, and at 10 times the concentration used in humans. Subsequently, blood tests were conducted and the development of pulmonary embolism was monitored by computed tomography (CT) tests. No incidents of pulmonary embolism due to the administration of mesenchymal cells were observed, and the method can be used safely.

Cold run at a cell-processing center for preparation of clinical study. Once the quality had been assessed, the cell culture was established in a cell-processing center (CPC) and monitored in compliance with the standard operating procedures. In addition, if the cell culture involved fetal bovine serum (FBS), tests for the detection of residual FBS in the cell preparations were conducted before the evaluations. This stage of the study is focused on assessing whether the cell culture method established outside the CPC can be adopted and used by the CPC. Currently, we are conducting simulations of the practicality of this method for application in humans.

Quality assessment and standard criteria. The quality of the cultured mesenchymal stem cells was examined using flow cytometry with cell-specific surface markers. Cultures were tested for sterility, mycoplasma contamination, and presence of endotoxins and viruses. In addition, if the cell culture involved FBS, the cell preparations were analyzed for residual FBS before further evaluations.

Preparation and realization of a clinical research proposal. We plan to make our clinical research proposal comparable to those already implemented for treating cirrhosis patients who have already been treated with the ABM*i* therapy. In addition, we plan to conduct experiments with cultured mesenchymal cells in accordance with the image shown in Figure 3, starting with laboratory studies. We believe that sufficient amounts of cultured mesenchymal cells can be obtained from small volume aspirates taken under local anesthesia, and that those cell numbers will be higher than those in the currently obtained 30-mL bone marrow aspirates. In addition, the cells can be preserved after culturing and thus can be administered frequently (Fig. 3). This procedure may induce gradual repair and regeneration of the liver and progression from the decompensated cirrhosis to the cirrhosis state and later to the hepatitis state.

Future Prospects

The ABM*i* therapy developed for treating liver cirrhosis has been officially approved as an "Advanced medical technology B" in Japan. In future, we plan to further investigate the ABM*i* therapy by conducting randomized and multicenter clinical studies and gather more evidence. We are also preparing clinical studies on regenerative therapy by using small amounts of the next-generation BMCs (harvested through minimally invasive bone marrow aspiration) based on our previous laboratory and clinical research. A

therapeutic approach based on using somatic stem cells such as cultured BMCs for the treatment of liver cirrhosis is urgently needed. The development of such a strategy will firmly establish an effective regenerative therapy for the treatment of liver cirrhosis, potentially saving the lives of many patients.

Acknowledgments

This study was supported by Grants-in-Aid for scientific research from the Japan Society for the Promotion of Science (JSPS); the Ministry of Health, Labour and Welfare, Health and Labour sciences research grants; and the Japan Science and Technology Agency (JST), the project of realization of regenerative medicine and highway.

Disclosure Statement

No competing financial interests exist.

References

1. Theise, N.D., Badve, S., Saxena, R., Henegariu, O., Sell, S., Crawford, J.M., and Krause, D.S. Derivation of hepatocytes from BMCs in mice after radiation-induced myeloablation. Hepatology **31,** 235, 2000.
2. Terai, S., Sakaida, I., Yamamoto, N., Omori, K., Watanabe, T., Ohata, S., Katada, T., *et al.* An *in vivo* model for monitoring trans-differentiation of BMCs into functional hepatocytes. J Biochem (Tokyo) **13,** 551, 2003.
3. Terai, S., Sakaida, I., Nishina, H., and Okita, K. Lesson from the GFP/CCl4 model—translational research project: the development of cell therapy using autologous BMCs in patients with liver cirrhosis. J Hepatobiliary Pancreat Surg **12,** 203, 2005.
4. Sakaida, I., Terai, S., Yamamoto, N., Aoyama, K., Ishikawa, T., Nishina, H., and Okita, K. Transplantation of BMCs reduces CCl4-induced liver fibrosis in mice. Hepatology **40,** 1304, 2004.
5. Iimuro, Y., Nishio, T., Morimoto, T., Nitta, T., Stefanovic, B., Choi, S.K., Brenner, D.A., *et al.* Delivery of matrix metalloproteinase-1 attenuates established liver fibrosis in the rat. Gastroenterology **124,** 445, 2003.
6. Higashiyama, R., Inagaki, Y., Hong, Y.Y., Kushida, M., Nakao, S., Niioka, M., Watanabe, T., *et al.* Bone marrow-derived cells express matrix metalloproteinases and contribute to regression of liver fibrosis in mice. Hepatology **45,** 213, 2007.
7. Siller-Lopez, F., Sandoval. A., Salgado, S., Salazar, A., Bueno, M., Garcia, J., Vera, J., *et al.* Treatment with human metalloproteinase-8 gene delivery ameliorates experimental rat liver cirrhosis. Gastroenterology **126,** 1122, 2004;
8. Terai, S., Ishikawa, T., Omori, K., Aoyama, K., Marumoto, Y., Urata, Y., Yokoyama, Y., *et al.* Improved liver function in patients with liver cirrhosis after autologous bone marrow cell infusion therapy. Stem Cells **24,** 2292, 2006.
9. Kim, J.K., Park, Y.N., Kim, J.S., Park, M.S., Paik, Y.H., Seok, J.Y., Chung, Y.E., *et al.* Autologous bone marrow infusion activates the progenitor cell compartment in patients with advanced liver cirrhosis. Cell Transplant **19,** 1237, 2010.
10. Saito, T., Okumoto, K., Haga, H., Nishise, Y., Ishii, R., Sato, C., Watanabe, H., *et al.* Potential therapeutic application of intravenous autologous bone marrow infusion in patients with alcoholic liver cirrhosis. Stem Cells Dev **20,** 1503, 2011.
11. Mizunaga, Y., Terai, S., Yamamoto, N., Uchida, K., Yamasaki, T., Nishina, H., Fujita, Y., Shinoda, K., Hamamoto, Y., and Sakaida, I. Granulocyte colony-stimulating factor and interleukin-1β are important cytokine in repair of the cirrhotic liver after bone marrow cell infusion—comparison of humans and model mice. Cell Transplant **21,** 2363, 2012.
12. Iwamoto, T., Tera, S., Mizunaga, Y., Yamamoto, N., Omori, K., Uchida, K., Yamasaki, T., *et al.* Splenectomy enhances the anti-fibrotic effect of bone marrow cell infusion and improves liver function in cirrhotic mice and patients. J Gastroenterol **47,** 300, 2012.
13. Gholamrezanezhad, A., Mirpour, S., Bagheri, M., Mohamadnejad, M., Alimoghaddam, K., Abdolahzadeh, L., Saghari, M., *et al. In vivo* tracking of 111In-oxine labeled mesenchymal stem cells following infusion in patients with advanced cirrhosis. Nucl Med Biol **38,** 961, 2011.
14. Peng, L., Xie, D.Y., Lin, B.L., Liu, J., Zhu, H.P., Xie, C., Zheng, Y.B., *et al.* Autologous bone marrow mesenchymal stem cell transplantation in liver failure patients caused by hepatitis B: short-term and long-term outcomes. Hepatology **54,** 820, 2011.
15. Maeda, M., Takami, T., Terai, S., and Sakaida, I. Autologous bone marrow cell infusions suppress tumor initiation in hepatocarcinogenic mice with liver cirrhosis. J Gastroenterol Hepatol **27 Suppl 2,** 104, 2012.
16. Terai, S., Tanimoto, H., Maed, M., Zaitsu, J., Hisanaga, T., Iwamoto, T., Fujisawa, K., *et al.* Timeline for development of autologous bone marrow infusion (ABMi) therapy and perspective for future stem cell therapy. J Gastroenterol **47,** 491, 2012.
17. Mohamadnejad, M., Namiri, M., Bagheri, M., Hashemi, S.M., Ghanaati, H., Zare Mehrjardi, N., Kazemi Ashtiani, S., *et al.* Phase 1 human trial of autologous bone marrow-hematopoietic stem cell transplantation in patients with decompensated cirrhosis. World J Gastroenterol **13,** 3359, 2007.
18. Tanimoto, H., Terai, S., Takami, T., Murata, Y., Fujisawa, K., Yamamoto, N., and Sakaida, I. Improvement of liver fibrosis by infusion of cultured cells derived from human bone marrow. Cell Tissue Res **354,** 717, 2013.

Address correspondence to:
Shuji Terai, MD, PhD
Department of Gastroenterology and Hepatology
Yamaguchi University Graduate School of Medicine
Minami-kogushi 1-1-1, Ube
Yamaguchi 755-8505
Japan

E-mail: terais@yamaguchi-u.ac.jp

Received: August 28, 2013
Accepted: January 8, 2014
Online Publication Date: March 5, 2014

Am J Physiol Gastrointest Liver Physiol 307: G50–G57, 2014.
First published May 8, 2014; doi:10.1152/ajpgi.00434.2013.

Epiregulin promotes the emergence and proliferation of adult liver progenitor cells

Kyoko Tomita,[1,2] Hiroaki Haga,[1] Kei Mizuno,[1,2] Tomohiro Katsumi,[1] Chikako Sato,[1,2] Kazuo Okumoto,[1] Yuko Nishise,[1] Hisayoshi Watanabe,[1,2] Takafumi Saito,[1] and Yoshiyuki Ueno[1,2]

[1]*Department of Gastroenterology, Yamagata University Faculty of Medicine, Yamagata, Japan;* [2]*CREST, Yamagata University Faculty of Medicine, Yamagata, Japan*

Submitted 13 December 2013; accepted in final form 1 May 2014

Tomita K, Haga H, Mizuno K, Katsumi T, Sato C, Okumoto K, Nishise Y, Watanabe H, Saito T, Ueno Y. Epiregulin promotes the emergence and proliferation of adult liver progenitor cells. *Am J Physiol Gastrointest Liver Physiol* 307: G50–G57, 2014. First published May 8, 2014; doi:10.1152/ajpgi.00434.2013.—We have previously reported that epiregulin is a growth factor that seems to act on liver progenitor cells (LPCs) during liver regeneration. However, the relationship between epiregulin and LPCs has remained unclear. The aim of the present study was to clarify the role of epiregulin during liver regeneration. The serum levels of epiregulin in patients with acute liver failure were examined. A liver injury model was developed using mice fed a diet containing 0.1% 3.5-diethoxycarbonyl-1.4-dihydrocollidine (DDC) to induce LPCs. We then evaluated the expression of epiregulin and LPCs in these mice. The proliferation of epithelial cell adhesion molecule + LPCs cultured with epiregulin was examined in vitro, and finally epiregulin was overexpressed in mouse liver. In patients with acute liver failure, serum epiregulin levels were elevated significantly. In DDC mice, LPCs emerged around the portal area. Epiregulin was also detected around the portal area during the course of DDC-induced liver injury and was partially coexpressed with Thy1. Serum epiregulin levels in DDC mice were also significantly elevated. Recombinant epiregulin augmented the proliferative capacity of the LPCs in a dose-dependent manner. In mice showing overexpression of epiregulin, the expression of PCNA on hepatocytes was increased significantly. Finally, LPCs emerged around the portal area after epiregulin gene delivery. We concluded that epiregulin promotes the proliferation of LPCs and DNA synthesis by hepatocytes and is upregulated in the serum of patients with liver injury. Furthermore, induction of epiregulin leads to the appearance of LPCs. Epiregulin would be a useful biomarker of liver regeneration.

liver regeneration; progenitor cells; epiregulin; epithelial cell adhesion molecule; Thy1; liver injury

CURRENTLY, LIVER TRANSPLANTATION is the only therapeutic option for rescue of patients with end-stage liver disease. However, the shortage of organ donors has limited its application for most patients, including those in Japan, suggesting the need for an alternative therapeutic option. One such promising option for liver regeneration is cellular transplantation, using resources such as pluripotent stem cells, embryonic stem cells, umbilical cord blood cells, bone marrow cells (BMCs), liver cells, and liver progenitor cells (LPCs). We have been focusing on BMCs and LPCs, the former having been shown to be capable of differentiating into the liver cell lineage under a variety of conditions (2, 16, 23). When liver injury occurs, the stem cells among BMCs subsequently engraft and differentiate, thus contributing to regeneration (24). Recently, autologous BMC transplantation (a technique known as autologous BMC infusion therapy) has been applied for patients with liver cirrhosis and is reported to improve the serum levels of albumin and total protein, leading to an improvement of the Child-Pugh score (22). We have also applied this autologous BMC infusion therapy for patients with alcoholic cirrhosis, resulting in successful improvement of liver function (18).

Previously, we have demonstrated the differentiation of LPCs into hepatocytes during coculture with BMCs. Moreover, fibroblast growth factor (FGF) 2 has been shown to be a critical factor for this LPC migration (8). Gene expression analysis using a cDNA microarray on BMCs under coculture with LPCs demonstrated upregulated gene expression of various other growth factors. Among these growth factors, we have focused on epiregulin, a growth factor that was upregulated along with FGF2.

Epiregulin, first isolated from a fibroblast-derived cancer cell line in 1995 (26), is a membrane-bound growth factor belonging the epidermal growth factor (EGF) family, which binds to and activates both the EGF receptor (EGFR) and erythroblastic leukemia viral oncogene homolog-4 (ErbB4) (11). A few studies have focused on the role of epiregulin during regeneration. Komurasaki et al. (12) reported that epiregulin promoted the proliferation of primary cultured hepatocytes in vitro and that the epiregulin gene was upregulated at 24 and 48 h after partial hepatectomy (PH) in a rat model. However, the precise relationship between epiregulin and its effects on LPCs has remained unclear.

In general, two mechanisms of liver regeneration operate: *1*) after PH, residual mature hepatocytes restore the liver mass volume (13); *2*) in cases of severe liver injury where the proliferation of residual mature hepatocytes is limited, the LPCs are activated and then proliferate and differentiate, thus contributing to liver regeneration (7). The latter pattern of regeneration involving LPCs is more important in patients with advanced liver failure. However, the precise mechanism of LPC-dependent regeneration, including the effect of epiregulin, remains unclear.

The aim of the present study was to clarify the role of epiregulin during liver regeneration using a mouse model. Our results suggested that epiregulin plays a role in liver regeneration by promoting cellular proliferation and the emergence of LPCs.

MATERIALS AND METHODS

Animals. C57BL/6J mice (CLEA, Tokyo, Japan) were used for all the experiments. All animals were maintained under standard

Address for reprint requests and other correspondence: K. Tomita, MD, Dept. of Gastroenterology, Yamagata Univ. Faculty of Medicine, 2-2-2 Iida-nishi, Yamagata 990-9585, Japan (e-mail: to.kyoko@med.id.yamagata-u.ac.jp).

Table 1. *Patients' characteristics*

	Acute Liver Failure, n = 14	Acute Hepatitis, n = 24	Liver Cirrhosis, n = 24	Chronic Hepatitis, n = 24	Control, n = 24	P Value
Age, yr	47 ± 14.6	48.5 ± 12.2	48.1 ± 11.1	48.6 ± 12.9	48.8 ± 15.7	0.99
Sex, m/f	10/4	14/10	13/11	14/10	14/10	0.88
Total bilirubin, mg/dl	9.8[2.4–32.4]	3.8[0.4–40]	1.7 ± 1.2	0.9 ± 0.3	0.7 ± 0.4	$P < 0.05$
AST, IU/l	1111[82–6335]	557[38–7403]	45[16–192]	32[16–122]	20.6 ± 5.6	$P < 0.05$
ALT, IU/l	1377[37–5690]	545[56–4640]	31[8–122]	38[13–129]	17.7 ± 6.5	$P < 0.05$
Plt, 1.0 × 103/μl	11 ± 6.8	23.3 ± 10.2	11.6 ± 7.5	18.2 ± 5.1	25.6 ± 8.7	$P < 0.05$
PT, %	33.7 ± 10.6	92.8 ± 28.2	68.8 ± 18.8	107.2 ± 8.9	—	$P < 0.05$
PT-INR	1.9 ± 0.3	1.08 ± 0.18	1.27 ± 0.24	0.65 ± 0.05	—	$P < 0.05$
Etiology						
HBV/HCV/AIH/PBC/	3/0/2/0/	7/1/3/0/	2/8/2/1/	7/15/0/0/		
Alcohol/Drug/NAFLD/	4/3/0/	4/3/0/	6/0/2/	1/1/0/		
Other/Unknown	0/2	4/2	3/0	0/0	—	

Applicable values are presented as means ± SD or median[range]. AST, aspartate aminotransferase; ALT, alanine aminotransferase; Plt, platelets; PT, prothrombin time; PT-INR, prothrombin time and international normalized ratio; HBV, hepatitis B virus; HCV, hepatitis C virus; AIH, autoimmune hepatitis; PBC, primary biliary cirrhosis; NAFLD; nonalcoholic fatty liver disease.

SPF conditions, and all the experiments using animals were performed under institutional guidelines. Mouse liver progenitor cells were induced by feeding 8-wk-old male mice a diet containing 0.1% 3.5-diethoxycarbonyl-1.4-dihydrocollidine (DDC) (CLEA). In a gene-delivery experiment involving hydrodynamic tail vein injection (HTVi), male mice weighing 18–20 g were used. The experiments involving both gene delivery and animals were approved by the institutional review board (animal experiment; approval number 24139, gene-splicing research; approval number 24-27).

Gene delivery. A plasmid in which mouse epiregulin cDNA was cloned into the pLIVE (Liver in Vivo Expression) vector and the empty expression pLIVE vector (Mirus Bio, Madison, WI) were purchased from Takara (Shiga, Japan). The mouse epiregulin plasmid was amplified by *Escherichia coli* DH5α competent cells (Takara) and purified using an Endofree Plasmid Mxi Kit (Qiagen, Dusseldorf, Germany). Plasmid DNA was administered to mice using a HTVi technique involving rapid injection of a large volume of DNA solution through the tail vein. Briefly, 20 μg of plasmid DNA (1 mg/ml) was diluted in 2 ml of TransIT-EE Hydrodynamic Delivery Solution (Mirus Bio) and injected into male mice weighing 18–20 g via the tail vein within 6 to 8 s.

Immunohistochemistry. For immunohistochemistry (IHC), a rabbit polyclonal antibody against mouse CK19 (Proteintech, Chicago IL) and a rabbit polyclonal antibody against mouse epiregulin (Abbiotec, San Diego, CA) were used at a dilution of 1:50. A mouse monoclonal antibody against PCNA (clone PC-10; Nichirei, Tokyo, Japan), a rat monoclonal antibody against mouse epithelial cell adhesion molecule (EpCAM) (BD Pharmingen, San Diego, CA), and a rat monoclonal antibody against mouse Thy1 (BD Pharmingen) were used at a dilution of 1:100. The formalin-fixed paraffin-embedded liver sections (3 μm) underwent antigen retrieval processing in a microwave oven after deparaffinization. After being blocked with blocking one Histo reagent (Nakarai, Kyoto, Japan), the samples were incubated with primary antibodies and subsequently with high-molecular-weight polymer secondary antibodies (Simple Stain kit, Nichirei). The samples were finally developed with a peroxidase substrate ImmPACT NovaRED kit (Vector Laboratories, Burlingame, CA). Frozen sections (6 μm) from the liver were placed on APS-coated glass slides using a cryostat (Leica CM 3050S). After being fixed with ethanol, the samples were incubated with the primary antibodies and then incubated with fluorescence-conjugated secondary antibodies before observation by fluorescence microscopy (D1; Zeiss Axio Observer, Jena, Germany).

RNA extraction and RT-PCR. Total RNA was extracted from cells and tissues using a RNeasy Plus Mini Kit (Qiagen). Total RNA (2 μg) was used to synthesize cDNA using a SuperScript VILO cDNA synthesis kit (Life Technologies, Carlsbad, CA). The samples were subjected to 40 cycles of denaturation at 94°C for 30 s, annealing at 58°C for 30 s, and extension at 72°C for 30 s. PCR primers for mouse genes were as follows (5′ to 3′): *1*) epiregulin, TTGGGTCTTGACGCTGCTTTGT and TGAGGTCACTCTCATATTC; *2*) EGFR, CTGCCAAGGCACAAGTAACA and ATTGGGACAGCTTGGATCAC; *3*) Erbb4, GCTGAGGAATATTTGGTCCCCCAG and AAACATCTCAGCCGTTGCACCCTG; *4*) β-actin, GGCTGTATTCCCCTCCATCG and CCAGTTGGTAATGCCATGT. Quantitative real-time PCR was performed using a 7500 Real-Time PCR system (Applied Biosystems, Foster City, CA) with the TaqMan Gene Expression Assay (Assay ID): epiregulin, Mm00514794_m1; and GAPDH, Mm99999915_g1.

Cell culture and proliferation assay. An EpCAM-positive liver progenitor cell line from the liver of a DDC-fed adult mouse was kindly provided by Dr. Atsushi Miyajima (Laboratory of Cell Growth and Differentiation, Institute of Molecular and Cellular Biosciences, The University of Tokyo). The EpCAM+ cells were maintained in a cell culture flask (Corningware, Corning, NY) using medium supplemented with fetal bovine serum and 10 ng/ml of each human recombinant EGF and hepatocyte growth factor (HGF). The proliferative response of EpCAM+ cells was exam-

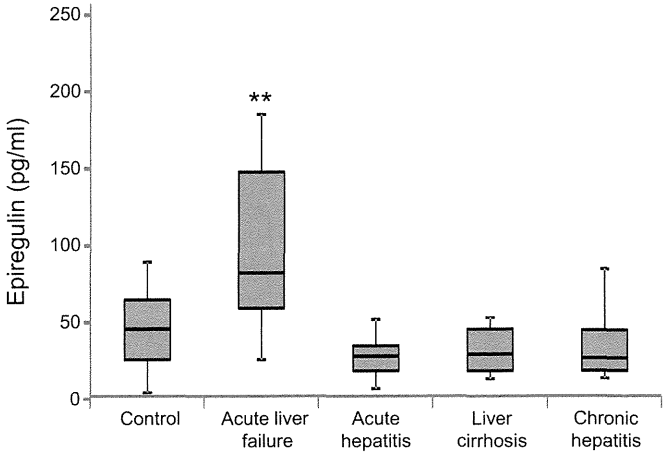

Fig. 1. ELISA for determination of human epiregulin was performed on serum samples from healthy controls (n = 25) and patients with acute liver failure (n = 14), acute hepatitis (n = 24), liver cirrhosis (n = 24), and chronic hepatitis (n = 24). Acute liver failure was defined as severe liver dysfunction, as indicated by a prothrombin time of less than 40% or prothrombin time and international normalized ratio (commonly called PT-INR) >1.5 within 8 wk after initial presentation of symptoms. Serum epiregulin levels in patients with acute liver failure were significantly higher than those in healthy controls. However, there were no significant differences among the other disease groups. Means ± SD, $^{**}P < 0.01$.

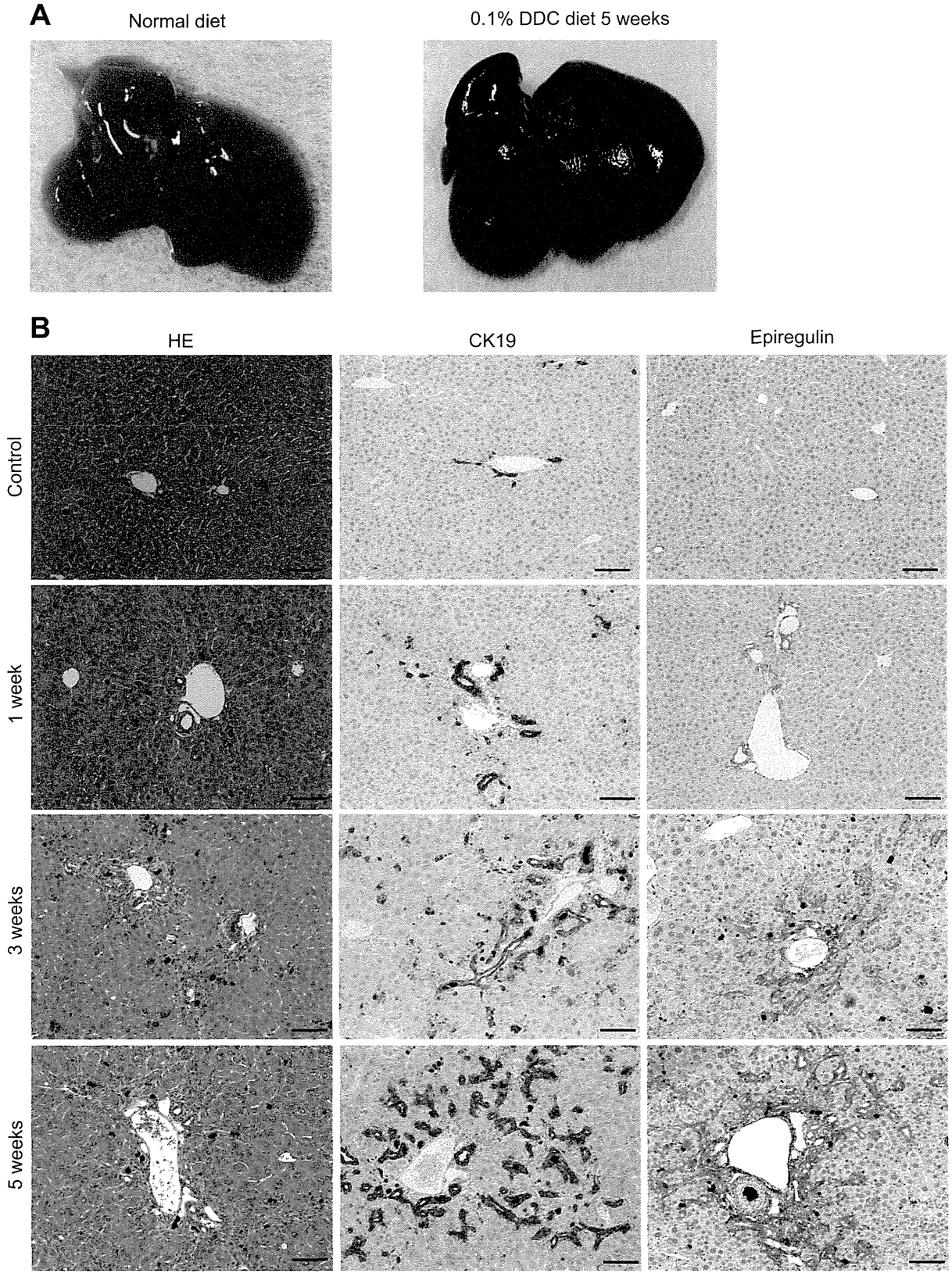

Fig. 2. Mouse liver progenitor cells (LPCs) were induced by a diet containing 0.1% 3.5-diethoxycarbonyl-1.4-dihydrocollidine (DDC) in C57BL/6J mice. *A*: liver turned black and stiff after 5 wk on the DDC diet. *B*: hematoxylin and eosin (HE) staining of livers from mice on the DDC diet demonstrated ductular proliferation consisting of small cells in the portal area from 1 to 5 wk. These small cells were positive for CK19, indicating that they were LPCs. The expression of epiregulin protein was markedly elevated around ductular structures close to the portal area during the course of DDC-induced liver injury. Bars = 100 μm.

ined in the presence of FBS, EGF, or HGF in different concentrations, using the water-soluble tetrazolium salt (WST)-1 cell proliferation reagent (Roche, Basel, Switzerland). The absorbance value (OD450-OD650) was measured using a Benchmark Plus microplate reader (Bio-Rad, Hercules, CA).

Serum epiregulin immunoassay. The human and mouse serum epiregulin values were measured using an epiregulin-specific ELISA (USCN, Hubei, China) in accordance with the manufacturer's protocol (assay range: 6.4–1,000 pg/ml). The absorbance value (450 nm) was measured using a Benchmark Plus microplate reader (Bio-Rad).

Statistical analysis. Comparison of gene expression assays, immunoassay, and patient background were done using one-way ANOVA with subsequent Steel-Dwass or Tukey-Kramer tests. Analysis of the cell proliferation assay was done using two-way ANOVA. Differences at $P < 0.05$ were considered to be statistically significant. The above statistical analyses were done using the SAS software package (SAS Institute, Cary, NC).

RESULTS

Elevation of serum epiregulin levels in patients with acute liver failure. To investigate whether epiregulin is involved in liver regeneration, we determined the serum epiregulin levels in patients with a variety of liver diseases, including acute liver failure, acute hepatitis, chronic hepatitis, and liver cirrhosis. Those in healthy subjects were also examined for comparison. Acute liver failure was defined as severe liver dysfunction with a prothrombin time of less than 40% or prothrombin time and international normalized ratio (commonly called PT-INR) >1.5 within 8 wk after initial presentation (14). There was no significant difference in background factors such as age or sex ratio between the groups. Other characteristics including the degree of liver damage are listed in Table 1. Serum epiregulin levels in patients with acute liver failure were significantly higher than in healthy controls (Fig. 1). However, there were no significant differences among the other disease groups. This observation may have reflected the promotion of epiregulin production only under conditions in which proliferation of normal hepatocytes would be limited.

Expression of epiregulin in injured adult mouse liver concomitant with LPC emergence. The 2-acetylaminofluorene (2-AAF)/PH model, in which hepatocyte proliferation is blocked by 2-AAF before PH, has been used to induce LPCs in rats (5, 6). Recently, a 0.1% DDC-containing diet has been developed to induce LPCs in mice, and this mouse model was employed for the present study (1, 17). After 4–5 wk on the DDC diet, the liver of mice appeared black and stiff (Fig. 2*A*). Hematoxylin and eosin staining was used to evaluate adult normal liver and liver with DDC-induced injury. After 1 wk on the DDC diet, the liver demonstrated ductular structures around the portal area, and these gradually increased up to 5 wk (Fig. 2*B*). These ductular structures consisted of small cells with large nuclei, with a so-called "oval cell" appearance. IHC for CK19, one of the markers of LPCs and cholangiocytes, showed that these small cells included CK19-expressing LPCs (Fig. 2*B*). Epiregulin protein expression was barely detectable in normal liver but was markedly induced around the ductular structures close to the portal area during the course of DDC-induced liver injury (Fig. 2*B*). Quantitative gene expression analysis confirmed that the expression of epiregulin mRNA was significantly increased in the DDC-injured liver after 4–5 wk on the DDC diet (Fig. 3, *A* and *B*). In addition, the serum epiregulin level was significantly increased from 2 wk on the DDC diet and gradually increased up to 4 wk (Fig. 3*C*).

Coexpression of epiregulin with Thy1-positive cells around ductular structures in injured mouse liver. To investigate the site of epiregulin expression, we examined injured mouse liver using IHC. As briefly mentioned above, IHC for CK19 and epiregulin confirmed that epiregulin was expressed around the LPCs forming ductular structures. Recently, as it has been reported that Thy1-positive cells express growth factors nec-

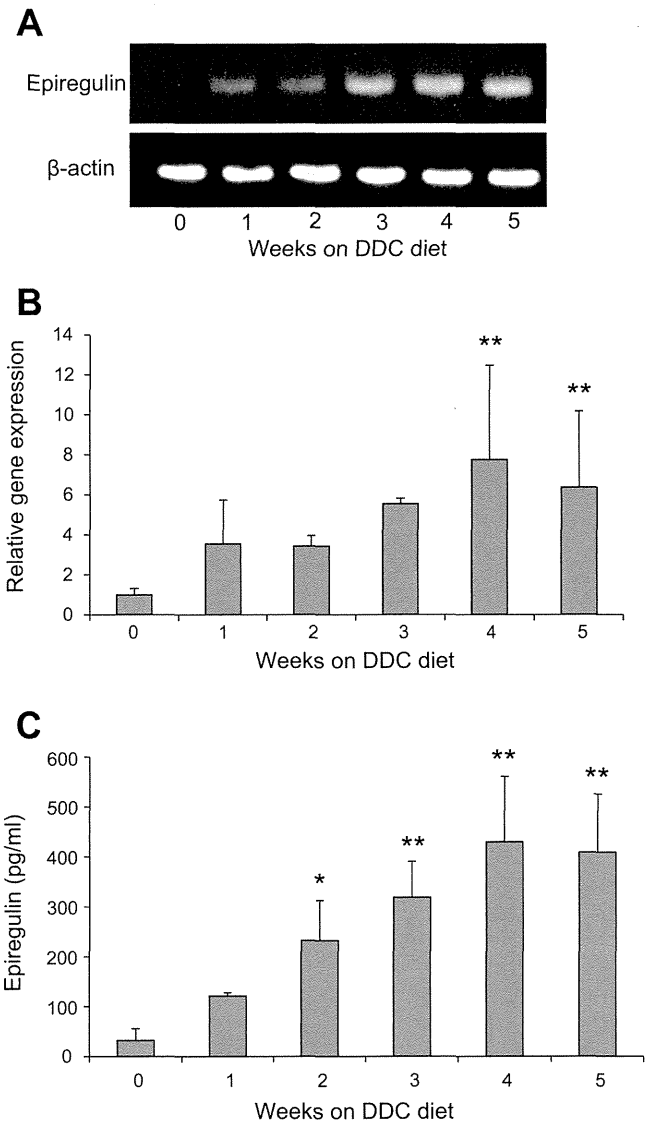

Fig. 3. Serum and hepatic epiregulin expression in DDC mice. *A*: RT-PCR for epiregulin mRNA in mouse liver after DDC diet feeding. The epiregulin gene was expressed from 1 to 5 wk after the start of the DDC diet. *B*: quantitative changes in the level of epiregulin mRNA in mouse liver after DDC diet feeding, determined by real-time PCR analysis. Epiregulin expression was normalized against that of GAPDH. Epiregulin mRNA was increased from 1 wk after the start of the DDC diet and was significantly increased at 4–5 wk relative to the value at 0 wk. Mean ± SD ($n = 3$). *C*: ELISA for serum epiregulin showed a significant increase from 2 wk after the start of DDC diet feeding and reached a peak at 4 wk relative to the value at 0 wk. Means ± SD ($n = 4$). $^{**}P < 0.01$, $^{*}P < 0.05$.

essary for the maintenance of LPCs (15), we performed IHC for epiregulin and Thy1, which are markers of mesenchymal cells or LPCs. First, we performed double immunostaining for CK19 and EpCAM as LPC markers and confirmed that both were coexpressed around ductular structures in the portal area at 5 wk. Double immunostaining for epiregulin and EpCAM revealed that epiregulin was expressed adjacent to the LPCs forming ductular structures. Further double immunostaining for Thy1 and epiregulin revealed partial coexpression of these two markers (Fig. 4).

Epiregulin promotes the proliferation of EpCAM+ LPCs in vitro. Because epiregulin was expressed close to LPCs in injured mouse liver, we performed an in vitro study to investigate whether epiregulin affects LPCs. First, to determine whether epiregulin acts on LPCs directly, we examined the expression of the epiregulin receptors EGFR and ErrbB4 in EpCAM+ LPCs. Although epiregulin is known to bind to and activate both EGFR and Erbb4 (11), only EGFR was expressed in EpCAM+ LPCs (Fig. 4*A*). Subsequently, we examined the proliferation of LPCs under different dosages of either recombinant epiregulin or EGF, another EGFR ligand. EpCAM+ LPCs were exposed to 0, 20, or 100 ng/ml epiregulin or EGF in culture, and their proliferations were measured after 3 days of incubation in 96-well plates using the standard WST-1 assay. This revealed that recombinant epiregulin promoted the proliferation of EpCAM+ LPCs in a concentration-dependent manner, and the proliferation efficacy was significantly higher in epiregulin than EGF (Fig. 4*B*).

Epiregulin overexpression in adult mouse liver induces LPCs and promotes the synthesis of DNA in hepatocytes. To investigate the effect of epiregulin on hepatocytes, the epiregulin gene was overexpressed in mice using the HTVi method, which involves injection of plasmid DNA via a tail vein and facilitates overexpression of the target gene in organs including the liver. Since Zhang et al. (19, 31) first reported the HTVi method in 1997, it has been used in various gene overexpression studies because of its *1*) high transfer efficiency and reproducibility and *2*) easier preparation of plasmid DNA (30). The epiregulin-overexpressing mice were killed at 3, 7, 14, and 21 days after gene delivery. The control mice were injected with empty expression plasmid vector. IHC for epiregulin confirmed its expression in the entire liver up to 21 days after gene delivery, reaching a peak during the initial 3–7 days (Fig. 6*A*). Empty vector-injected mice livers demonstrated no detectable levels of epiregulin expression. To evaluate DNA synthesis, IHC for PCNA was performed on epiregulin-overexpressing mouse liver. IHC for CK19 confirmed that LPC induction was evident from 3 days after epiregulin gene delivery (Fig. 5*A*). Furthermore, the ratio of PCNA-positive cells was increased significantly at 3, 7, and 14 days after epiregulin gene delivery (Fig. 6, *A* and *B*).

DISCUSSION

In the present study, we have shown that expression of epiregulin promoted the induction of LPCs and DNA synthesis by hepatocytes and that epiregulin was expressed by the stem cell niche including mesenchymal cells located around ductular structures in the portal area of adult mice. Furthermore, the serum epiregulin level was elevated in both patients and mice with liver injury. Taken together, these data suggested that

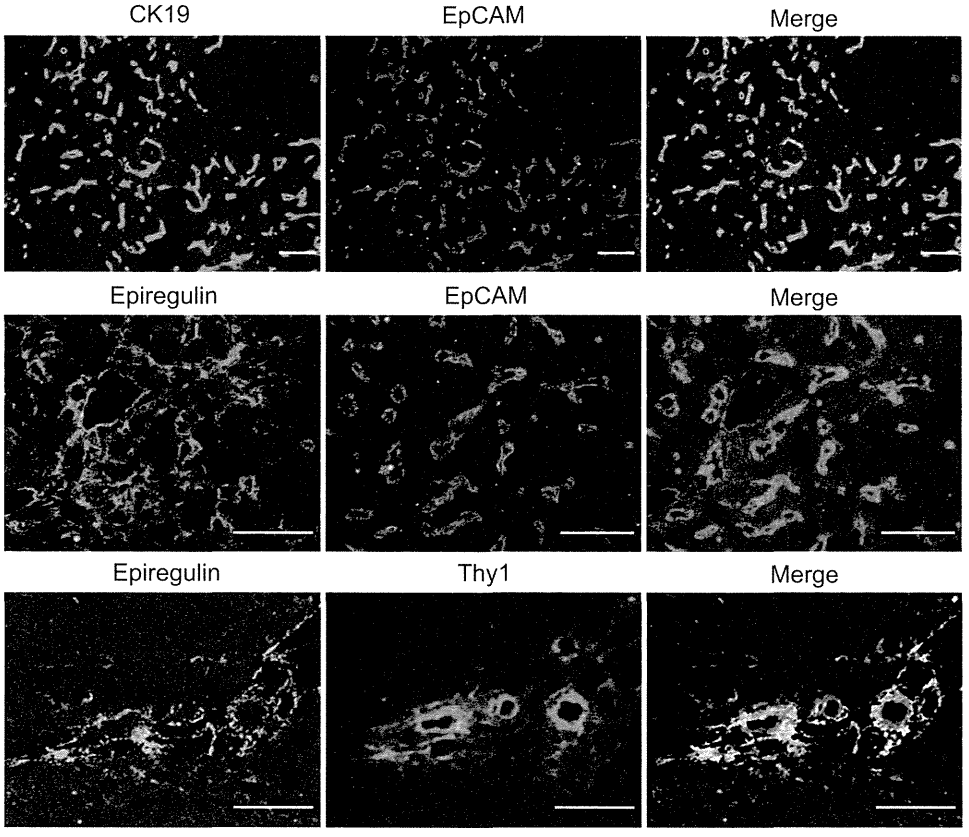

Fig. 4. Double immunostaining study of mouse liver after DDC diet feeding. First, we performed double immunostaining for CK19 and epithelial cell adhesion molecule (EpCAM) as LPC markers and confirmed that both markers were coexpressed and associated with ductular structures in the portal area of mice at 5 wk. Double immunostaining for epiregulin and EpCAM revealed that epiregulin was expressed adjacent to LPCs forming ductular structures. Further double immunostaining for Thy1 and epiregulin revealed partial coexpression of these 2 markers. Bar = 200 μm.

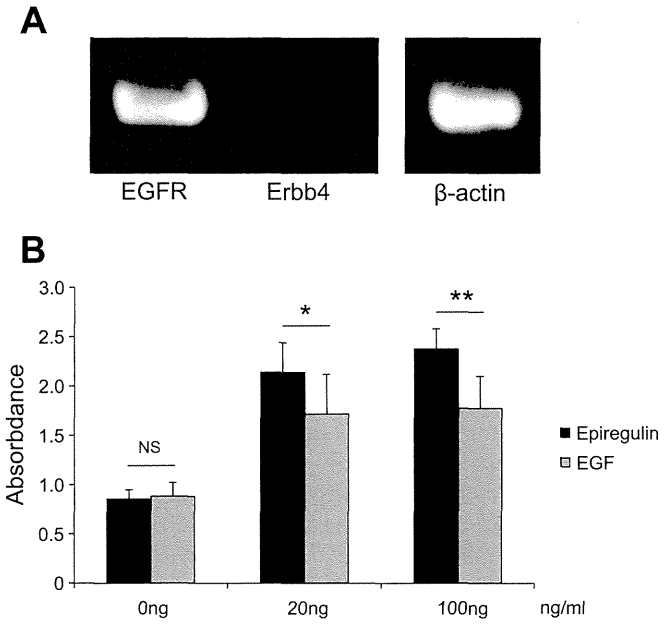

Fig. 5. Proliferation assay of LPCs cultured with recombinant epiregulin or epidermal growth factor (EGF). *A*: EGFR, but not ErrB4, was expressed in EpCAM+ LPCs. *B*: proliferation assay of LPCs cultured with recombinant epiregulin or EGF at 3 different concentrations (0, 20, 100 ng/ml). Recombinant epiregulin promoted the proliferation of EpCAM+ LPCs in a concentration-dependent manner. Furthermore, the proliferation efficacy was significantly higher in epiregulin than EGF. The water-soluble tetrazolium salt assay was repeated 8 times. Means ± SD, $^{**}P < 0.01$, $^{*}P < 0.05$.

active induction of epiregulin is required during liver regeneration to maintain homeostasis in vivo.

Komurasaki et al. (12) have reported that epiregulin promoted the proliferation of primary cultured hepatocytes in vitro and that its expression was upregulated after PH in rats. However, the precise relationship between epiregulin and LPCs has remained unclear. Furthermore, although epiregulin acts via the EGF receptor (11), neither its cells of origin nor the trigger for its expression have yet been proven. It is now known that LPCs originate from the canal of Hering and have bipotentiality for differentiation into either hepatocytes or cholangiocytes in injured adult liver (7). However, the mechanism of action and the origin of LPCs are still controversial.

Our study of the epiregulin level in human serum showed that it was significantly increased in patients with acute liver failure and did not differ significantly among several liver diseases, including acute hepatitis and cirrhosis. Epiregulin protein expression was also increased in both the liver and serum of DDC-fed mice. These data collectively imply that the expression of epiregulin is limited to conditions associated with critical liver injury in which there is insufficient regeneration of residual hepatocytes. In other words, increased epiregulin expression is related to the emergence of LPCs. HGF and TGF-α are known to be increased in severe liver injury (25, 27), and here we confirmed for the first time that the serum epiregulin level was elevated in patients with acute liver failure. Epiregulin may therefore be a useful biomarker for monitoring or assessing patients with severe liver injury, as is the case for HGF, which has been used as a prognostic indicator in patients with severe liver injury (28).

Epiregulin was expressed from 1 wk on the DDC diet and then gradually increased, reaching a peak at 4–5 wk. This course of expression was identical to that of CK19+ in LPCs. We have also shown that epiregulin was expressed in the area of LPCs forming ductular structures, i.e., the so-called stem cell niche, and was partially coexpressed by Thy1-positive cells. It has been reported that immune cells or mesenchymal cells emerge around the LPCs (10, 21). Recently, FGF7, another growth factor, was shown to be expressed by Thy1-positive cells forming the stem cell niche and to contribute to the maintenance of liver regeneration (15). Taken together, the data suggest that epiregulin may also contribute to liver regeneration through expression by Thy1-positive cells, which belong to the LPC niche. However, because epiregulin was partially coexpressed with Thy1, other candidate epiregulin-producing cells may exist. In fact heparin-binding-EGF, a hepatocyte growth-promoting factor belonging to the EGF family, is expressed by both endothelial cells and Kupffer cells (9).

In our in vivo study of mice with epiregulin overexpression, we have confirmed that epiregulin promoted the synthesis of DNA by mature hepatocytes and did not affect LPCs alone. The present study is the first study describing the ability of epiregulin to promote DNA synthesis in vivo. EGF was originally characterized as a growth factor that binds to specific receptors on the cell surface, stimulating protein tyrosine kinase activity leading to cellular proliferation and DNA synthesis (3, 4, 29). However, the signaling potencies of epiregulin and EGF were considered to be different (12). In particular, epiregulin is reported to exhibit modest activating effects for EGFR and MAPK phosphorylation although activating effects of epiregulin were supposed to be prolonged compared with those of EGF (12). In our in vitro study, epiregulin promoted the proliferation of LPCs, and its efficacies were higher than EGF. This biological difference may be derived partially due to the weak activating capabilities of epiregulin, which in turn affected to prevent the negative downstream regulations.

In this study, although epiregulin was shown to promote the induction and proliferation of LPCs, further analysis will be needed to confirm whether epiregulin is really essential for LPC induction, perhaps employing epiregulin gene-knockout mice. Although epiregulin gene-knockout mice have already been established, there have been no reports indicating that they have developmental anomalies in the liver (20). Using these epiregulin-knockout mice fed a DDC diet, we were able to evaluate whether LPCs were induced. Further analyses will be needed to determine whether there are unspecified epiregulin-expressing cells that are Thy1 negative.

In conclusion, epiregulin *1*) is expressed in the stem cell niche, which includes mesenchymal cells around the LPCs during severe liver injury, *2*) contributes to liver regeneration by inducing LPCs, and *3*) promotes DNA synthesis by mature hepatocytes. In addition, the serum epiregulin level is significantly elevated in both patients and mice with liver injury. Taken together, these data indicate that epiregulin would be a useful biomarker of liver regeneration.

ACKNOWLEDGMENTS

The authors are grateful to Dr. A. Miyajima, Dr. M. Tanaka, and Dr. T. Ito (Laboratory of Cell Growth and Differentiation, Institute of Molecular and

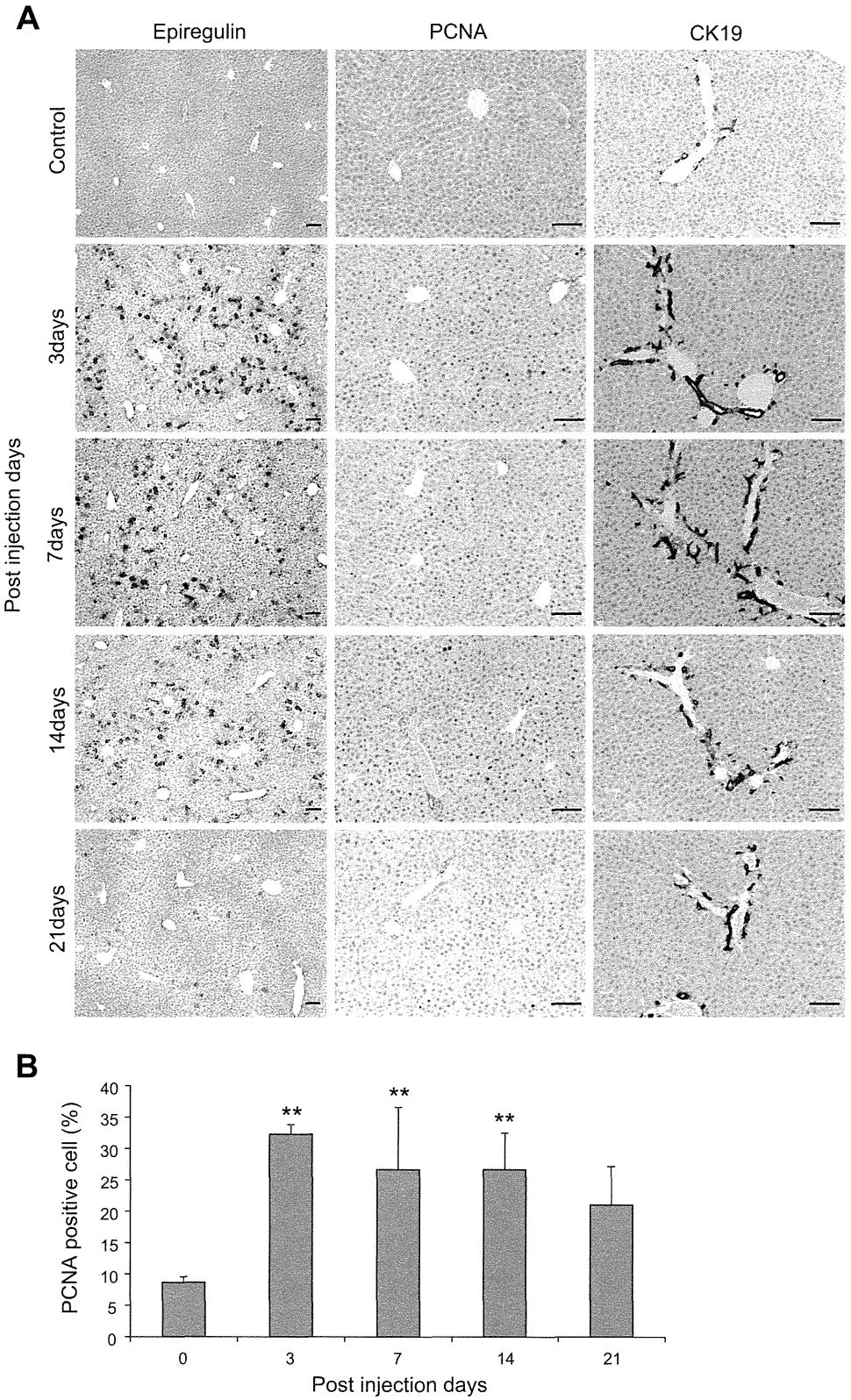

Fig. 6. The epiregulin gene was overexpressed using the hydrodynamic tail vein injection method in C57BL/6J mice. A: immunohistochemistry for epiregulin confirmed expression of the protein from 3 to 21 days after gene delivery. Control mice were studied 3 days after injection with empty expression plasmid vector. Along with epiregulin expression, the ratio of PCNA-positive cells was significantly increased at 3 to 14 days. In addition, ductular proliferation consisting of CK19-positive LPCs was confirmed at 3 to 21 days. Bar = 200 μm. *B*: ratio of PCNA-positive cells relative to the value in normal mice. The PCNA positivity ratio was significantly increased up to 14 days and peaked at 3 days after gene delivery. Means ± SD, $^{**}P < 0.01$.

Cellular Bioscience, The University of Tokyo) for providing the cell line and also their technical suggestions and to Dr. J. Yokozawa for technical assistance. Part of this study was presented at the annual meeting of the American Association for the Study of Liver Diseases, Washington DC, in November 2013.

GRANTS

This study was supported in part by Health and Labour Sciences Research Grants for Research on Measures for Intractable Diseases (from the Ministry of Health, Labour and Welfare of Japan).

DISCLOSURES

No conflicts of interest, financial or otherwise, are declared by the authors.

AUTHOR CONTRIBUTIONS

Author contributions: K.T., H.H., and Y.U. conception and design of research; K.T., H.H., K.M., and T.K. performed experiments; K.T. and H.H. analyzed data; K.T., H.H., K.M., T.K., C.S., K.O., Y.N., H.W., T.S., and Y.U. interpreted results of experiments; K.T. and H.H. prepared figures; K.T., H.H., and Y.U. drafted manuscript; K.T., H.H., and Y.U. edited and revised manuscript; K.T., H.H., and Y.U. approved final version of manuscript.

REFERENCES

1. **Akhurst B, Croager EJ, Farley-Roche CA, Ong JK, Dumble ML, Knight B, Yeoh GC.** A modified choline-deficient, ethionine-supplemented diet protocol effectively induces oval cells in mouse liver. *Hepatology* 34: 519–522, 2001.
2. **Alison MR, Poulsom R, Jeffery R, Dhillon AP, Quaglia A, Jacob J, Novelli M, Prentice G, Williamson J, Wright NA.** Hepatocytes from non-hepatic adult stem cells. *Nature* 406: 257, 2000.
3. **Boguski MS, McCormick F.** Proteins regulating Ras and its relatives. *Nature* 366: 643–654, 1993.
4. **Daum G, Eisenmann-Tappe I, Fries HW, Troppmair J, Rapp UR.** The ins and outs of Raf kinases. *Trends Biochem Sci* 19: 474–480, 1994.
5. **Evarts RP, Nagy P, Marsden E, Thorgeirsson SS.** A precursor product relationship exists between oval cells and hepatocytes in rat liver. *Carcinogenesis* 8: 1737–1740, 1987.
6. **Farber E.** Similarities in the sequence of early histological changes induced in the liver of the rat by ethionine, 2-acetylamino-fluorene, and 3'-methyl-4-dimethylaminoazobenzene. *Cancer Res* 16: 142–148, 1956.
7. **Fausto N.** Liver regeneration and repair: Hepatocytes, progenitor cells, and stem cells. *Hepatology* 39: 1477–1487, 2004.
8. **Haga H, Saito T, Okumoto K, Ugajin S, Sato C, Ishii R, Nishise Y, Ito J, Watanabe H, Saito K, Togashi H, Kawata S.** Enhanced expression of fibroblast growth factor 2 in bone marrow cells and its potential role in the differentiation of hepatic epithelial stem-like cells into the hepatocyte lineage. *Cell Tissue Res* 343: 371–378, 2011.
9. **Kiso S, Kawata S, Tamura S, Higashiyama S, Ito N, Tsushima H, Taniguchi N, Matsuzawa Y.** Role of heparin-binding epidermal growth factor-like growth factor as a hepatotrophic factor in rat-liver regeneration after partial hepatectomy. *Hepatology* 22: 1584–1590, 1995.
10. **Knight B, Akhurst B, Matthews VB, Ruddell RG, Ramm GA, Abraham LJ, Olvnyk JK, Yeoh GC.** Attenuated liver progenitor (oval) cell and fibrogenic responses to the choline-deficient, ethionine-supplemented diet in the BALB/c inbred strain of mice. *J Hepatol* 46: 134–141, 2007.
11. **Komurasaki T, Toyoda H, Uchida D, Morimoto S.** Epiregulin binds to epidermal growth factor receptor and ErbB-4 and induces tyrosine phosphorylation of epidermal growth factor receptor, ErbB-2, ErbB-3 and ErbB-4. *Oncogene* 15: 2841–2848, 1997.
12. **Komurasaki T, Toyoda T, Uchida D, Nemoto N.** Mechanism of growth promoting activity of epiregulin in primary cultures of rat hepatocytes. *Growth Factors* 20: 61–69, 2002.
13. **Michalopoulos GK, DeFrances MC.** Liver regeneration. *Science* 276: 60–66, 1997.
14. **Mochida S, Takikawa Y, Nakayama N, Oketani M, Naiki T, Yamagishi Y, Ichida T, Tsubouchi H.** Diagnostic criteria of acute liver failure: A report by the Intractable Hepato-Biliary Diseases Study Group of Japan. *Hepatol Res* 41: 805–812, 2011.
15. **Okabe M, Tsukahara Y, Tanaka M, Suzuki K, Saito S, Kamiya Y, Tsujimura T, Nakamura K, Miyajima A.** Potential hepatic stem cells reside in EpCAM(+) cells of normal and injured mouse liver. *Development* 136: 1951–1960, 2009.
16. **Petersen BE, Bowen WC, Patrene KD, Mars WM, Sullivan AK, Murase N, Boggs SS, Greenberger JS, Goff JP.** Bone marrow as a potential source of hepatic oval cells. *Science* 284: 1168–1170, 1999.
17. **Preisegger KH, Factor VM, Fuchsbichler A, Stumptner C, Denk H, Thorgeirsson SS.** Atypical ductular proliferation and its inhibition by transforming growth factor beta 1 in the 3,5-diethoxycarbonyl-1,4-dihydrocollidine mouse model for chronic alcoholic liver disease. *Lab Invest* 79: 103–109, 1999.
18. **Saito T, Okumoto K, Haga H, Nishise Y, Ishii R, Sato C, Watanabe H, Okada A, Ikeda M, Togashi H, Ishikawa T, Terai S, Sakaida I, Kawata S.** Potential therapeutic application of intravenous autologous bone marrow infusion in patients with alcoholic liver cirrhosis. *Stem Cells Dev* 20: 1503–1510, 2011.
19. **Sawyer GJ, Rela M, Davenport M, Whitehorne M, Zhang XH, Fabre JW.** Hydrodynamic gene delivery to the liver: Theoretical and practical issues for clinical application. *Curr Gene Ther* 9: 128–135, 2009.
20. **Shirasawa S, Sugiyama S, Baba I, Inokuchi J, Sekine S, Ogino K, Kawamura Y, Dohi T, Fujimoto M, Sasazuki T.** Dermatitis due to epiregulin deficiency and a critical role of epiregulin in immune-related responses of keratinocyte and macrophage. *Proc Natl Acad Sci USA* 101: 13921–13926, 2004.
21. **Strick-Marchand H, Masse GX, Weiss MC, Di Santo JP.** Lymphocytes support oval cell-dependent liver regeneration. *J Immunol* 181: 2764–2771, 2008.
22. **Terai S, Ishikawa T, Omori K, Aoyama K, Marumoto Y, Urata Y, Yokoyama Y, Uchida K, Yamasaki T, Fujii Y, Okita K, Sakaida I.** Improved liver function in patients with liver cirrhosis after autologous bone marrow cell infusion therapy. *Stem Cells* 24: 2292–2298, 2006.
23. **Theise ND, Badve S, Saxena R, Henegariu O, Sell S, Crawford JM, Krause DS.** Derivation of hepatocytes from bone marrow cells in mice after radiation-induced myeloablation. *Hepatology* 31: 235–240, 2000.
24. **Theise ND, Nimmakayalu M, Gardner R, Illei PB, Morgan G, Teperman L, Henegariu O, Krause DS.** Liver from bone marrow in humans. *Hepatology* 32: 11–16, 2000.
25. **Tomiya T, Fujiwara K.** Liver regeneration in fulminant hepatitis as evaluated by serum transforming growth factor alpha levels. *Hepatology* 23: 253–257, 1996.
26. **Toyoda H, Komurasaki T, Uchida D, Takayama Y, Isobe T, Okuyama T, Hanada K.** Epiregulin - a novel epidermal growth factor with mitogenic activity for rat primary hepatocytes. *J Biol Chem* 270: 7495–7500, 1995.
27. **Tsubouchi H, Gohda E, Strain AJ, Daikuhara Y.** The role of HGF-SF in animal and human hepatic physiology and pathology. *EXS* 65: 251–274, 1993.
28. **Tsubouchi H, Kawakami S, Hirono S, Miyazaki H, Kimoto M, Arima T, Sekiyama K, Yoshiba M, Arakaki N, Daikuhara Y.** Prediction of outcome in fulminant hepatic failure by serum human hepatocyte growth factor. *Lancet* 340: 307, 1992.
29. **Vandergeer P, Hunter T, Lindberg RA.** Receptor protein-tyrosine kinases and their signal-transduction pathways. *Annu Rev Cell Biol* 10: 251–337, 1994.
30. **Yang JW, Chen SP, Huang L, Michalopoulos GK, Liu YH.** Sustained expression of naked plasmid DNA encoding hepatocyte growth factor in mice promotes liver and overall body growth. *Hepatology* 33: 848–859, 2001.
31. **Zhang GF, Budker V, Wolff JA.** High levels of foreign gene expression in hepatocytes after tail vein injections of naked plasmid DNA. *Hum Gene Ther* 10: 1735–1737, 1999.

Hepatology Research

Hepatology Research 2014; 44: E26–E31 doi: 10.1111/hepr.12202

Original Article

Clinical manifestations of liver injury in patients with anorexia nervosa

Kyoko Tomita,[1] Hiroaki Haga,[1] Genki Ishii,[3] Tomohiro Katsumi,[1] Chikako Sato,[1,2] Rika Aso,[1] Kazuo Okumoto,[1] Yuko Nishise,[1] Hisayoshi Watanabe,[1,2] Takafumi Saito,[1] Koichi Otani[3] and Yoshiyuki Ueno[1,2]

[1]Department of Gastroenterology, [2]CREST, and [3]Department of Psychiatry, Yamagata University Faculty of Medicine, Yamagata, Japan

Aim: The number of Japanese patients with anorexia nervosa (AN) is increasing as society changes. Mild liver injury is a complication of AN in around 30% of cases. In some rare instances, patients present with severe liver injury similar to acute liver failure. However, there are numerous uncertainties over the clinical characteristics of this condition. The objective of the present study was to clarify the clinical characteristics of AN complicated by liver injury and to investigate the factors related to hepatic complications.

Methods: Thirty-seven patients hospitalized at our institution with a diagnosis of AN were enrolled as the study subjects. The study used clinical data obtained at the time of hospitalization. The enrolled patients underwent subgroup analysis and were categorized into three groups: (i) normal alanine aminotransferase (ALT), (ii) moderately elevated ALT, and (iii) highly elevated ALT.

Results: All of the study subjects were female with a median age of 24 years and presenting with marked weight loss (mean body mass index, 13 kg/m^2). Thirteen of the subjects had liver injury. We found that patients in the highly elevated ALT group had a significantly high blood urea nitrogen (BUN)/creatinine ratio, and a low blood sugar level.

Conclusions: Our present findings indicate that AN patients with highly elevated ALT have a severe dehydration. This suggests that dysfunction of hepatic circulation accompanying severe dehydration due to malnutrition may be an important factor in the development of liver injury in AN patients.

Key words: dehydration, eating disorder, emaciation, hypoxic hepatitis, liver enzyme

INTRODUCTION

ANOREXIA NERVOSA (AN) affects mainly adolescent females in developed countries including the USA, Europe and Japan. The majority of patients develop AN due to abnormal eating habits resulting from a desire to be lean or fear of becoming obese after exposure to psychiatric stress. In Japan, the prevalence of AN has been increasing rapidly;[1] according to annual reports issued by the Ministry of Health, Labour and Welfare, the incidence of eating disorders increased 10-fold in the 20 years since 1980, and the number of AN cases in particular increased fourfold during the 5 years since the mid 1990s. The prevailing explanation for this increase is the change of lifestyle in Japan including the increased variety of social circumstances. AN is associated with a number of complications including liver injury, especially elevation of the serum alanine aminotransferase (ALT) level in more than 30% of cases.[2] Furthermore, rare cases of severe liver injury resulting in acute liver failure have been reported.[3–5] However, the precise mechanism involved in the pathogenesis of liver injury associated with AN remains unclear. Moreover, few reports have documented the clinical features of AN complicated by liver injury. Some have indicated an association with low body mass index (BMI),[6,7] although the roles of other clinical surrogate markers are unclear.

The aim of the present study was to clarify the clinical features of AN complicated by liver injury and the

Correspondence: Dr Kyoko Tomita, Department of Gastroenterology, Yamagata University Faculty of Medicine, 2-2-2 Iida-nishi, Yamagata 990-9585, Japan. Email: mailto:to.kyoko@med.id.yamagata-u.ac.jp
Received 25 March 2013; revision 12 June 2013; accepted 7 July 2013.

clinical factors influencing hepatic complications. In clinical settings, it is important to predict the onset of severe liver injury associated with AN, which could be potentially life-threatening, and therefore it was anticipated that the information obtained from the present study would be of value to clinicians in assessing the risk of developing this serious complication.

METHODS

Study population

THIS RETROSPECTIVE OBSERVATION study was conducted between January 2010 and December 2011 at the Department of Gastroenterology and Department of Neuropsychiatry, Yamagata University Hospital. During this 2-year period, a total of 37 patients were admitted under a diagnosis of AN. These patients comprised both newly referred patients and established outpatients with exacerbation. There were also first admissions and repeat admissions due to deterioration of the patients' condition. The diagnosis of AN was made by a psychiatrist in accordance with the criteria of the Diagnostic and Statistical Manual of Mental Disorders, 4th edition (DSM-IV) on the basis of information obtained by interview from the patients and their families. The exclusion criteria were: (i) a history of hepatic disease, (ii) established infection with hepatitis viruses (HBV or HCV), (iii) drug abuse, (iv) excessive alcohol intake, and (v) presence of autoimmune liver disease. Especially for patients with highly elevated ALT, imaging studies (both ultrasound and dynamic CT scan) were performed to exclude other hepatobiliary diseases.

Study design

Clinical physiological parameters such as age, gender, BMI, body temperature, pulse rate, and blood pressure were evaluated, as well as routine laboratory data obtained on admission. Routine laboratory data included a complete blood cell count (CBC), hepatobiliary enzyme levels, renal function and blood sugar (BS) levels. The enrolled patients were subjected to subgroup analysis and categorized into three groups: (i) normal ALT defined as a serum ALT level of <42 IU/L, (ii) moderately elevated ALT defined as a serum ALT level between 42 IU/L and <840 IU/L (20 times above the institutional upper normal limit), and (iii) highly elevated ALT defined as a serum ALT level of >840 IU/L.

Statistical analysis

The above three subgroups were evaluated statistically by analysis of variance (ANOVA). If a significant difference was found, multiple comparisons (post hoc test) were performed with Tukey–Kramer and Steel–Dwass test. The risk related to elevated ALT was analyzed by univariate and multivariate logistic regression. The results of logistic regression analysis were expressed as odds ratio with 95% confidence interval. Differences after these modifications were considered significant at $P < 0.05$. Analyses were performed by using Excel Statistics (2010, Social Survey Research Information, Tokyo, Japan).

RESULTS

Patient features

THE BACKGROUNDS OF the 37 enrolled patients are listed in Table 1. The ages of the patients ranged from 12 to 67 years (median age 24 years), and all were lean females with a mean BMI on admission of 13 kg/m^2. The serum ALT level ranged widely from 11 to 2321 IU/L, with a median of 27 IU/L. Besides liver injury, physiological and laboratory abnormalities frequently associated with AN, such as bradycardia, hypothermia, hypotension, anemia, leukopenia, thrombocytopenia, hyponatremia, hypokalemia, and hypoglycemia were present in some of the enrolled patients.

Comparison of each clinical parameter according to the ALT level

Elevated liver enzyme (serum ALT level ≥42 IU/L) was observed in 13 (35%) of the 37 cases. Highly elevated ALT was evident in four cases (11%), the median ALT level being 1986.5 IU/L. Patients in the moderately elevated ALT group accounted for 24% of the subjects overall (9/37), and the median ALT level was 71 IU/L. The median serum ALT level in the normal ALT group was 20.5 IU/L. The clinical parameters in these three groups are detailed in Table 2. Among the clinical parameters evaluated, body temperature, pulse rate, blood urea nitrogen (BUN), BUN/creatinine ratio, BS, and platelet count differed significantly among the groups ($P < 0.05$). These six parameters were further analyzed statistically, and this revealed that both BUN and the BUN/creatinine ratio were significantly higher in the high ALT group than in the normal ALT ($P < 0.05$) and moderate ALT ($P < 0.05$) groups, respectively (Fig. 1). Body temperature, BS and platelet count were

Table 1 Characteristics of study population ($n = 37$)

Parameter	Mean ± SD	Range
Age (years)†	24	12–67
BMI (kg/m^2)	13.0 ± 2.2	9.5–17.9
Body temperature (°C)	36.5 ± 0.7	34.5–38.0
Pulse rate (bpm)	72.1 ± 19.8	46–111
Systolic blood pressure (mmHg)	95.8 ± 18.0	67–153
Diastolic blood pressure (mmHg)	63.2 ± 15.3	33–101
Albumin (g/dL)	4.4 ± 0.9	2.6–5.7
Total bilirubin (mg/dL)†	0.9	0.2–7.3
AST (IU/L)†	29	12–2628
ALT (IU/L)†	27	11–2321
BUN (mg/dL)	19.8 ± 11.3	4–47
Creatinine (mg/dL)†	0.66	0.16–1.57
BUN/creatinine (ratio)†	24.3	8–104.4
Na (mEq/L)†	140	121–146
K (mEq/L)	3.7 ± 0.6	2.4–5.1
Cl (mEq/L)	99.8 ± 6.8	76–110
Blood sugar (mg/dL)†	81	12–150
White blood cells (/μL)	5132.9 ± 2564.7	1 820–15 600
Hemoglobin (g/dL)	12.6 ± 2.0	5.7–16.5
Platelet count (/μL)	23.6 ± 9.2	8.1–41.1

†Median.
ALT, alanine aminotransferase; AST, aspartate aminotransferase; BMI, body mass index; BUN, blood urea nitrogen; SD, standard deviation.

Table 2 Comparison of each clinical parameter according to the alanine aminotransferase (ALT) level

Parameter	Highly elevated ALT group (ALT ≥ 840) $n = 4$	Moderately elevated ALT group (840 > ALT ≥ 42) $n = 9$	Normal ALT group (ALT < 42) $n = 24$	*P*-value
Age (years); median [range]	17 [16–31]	29 [13–50]	22 [12–67]	0.495
BMI (kg/m^2); mean ± SD	10.7 ± 1.1	13.4 ± 3.0	13.3 ± 1.8	0.070
Body temperature (°C); mean ± SD	35.3 ± 0.9	36.8 ± 0.5	36.7 ± 0.7	<0.05
Pulse rate (bpm); mean ± SD	50.5 ± 12.2	67.7 ± 15.7	75.9 ± 20.1	<0.05
Systolic blood pressure (mmHg); mean ± SD	92.3 ± 12.1	97.7 ± 11.6	95.7 ± 20.9	0.890
Albumin (g/dL); mean ± SD	4.4 ± 0.6	3.9 ± 1.0	4.6 ± 0.8	0.110
AST (IU/L); median [range]	2249.5 [1684–2628]	68 [39–512]	22 [12–53]	<0.05
ALT (IU/L); median [range]	986.5 [871–2321]	71 [48–215]	20.5 [11–36]	<0.05
BUN (mg/dL); mean ± SD	41.0 ± 6.1	17.4 ± 9.9	17.1 ± 8.6	<0.05
Creatinine (mg/dL); median [range]	0.64 [0.45–0.67]	0.56 [0.35–0.7]	0.71 [0.16–1.57]	0.062
BUN/creatinine; median [range] (ratio)	63.6 [53.2–104.4]	28.3 [11.6–56.9]	19.4 [8–68.6]	<0.05
Na (mEq/L); mean ± SD	141.0 ± 5.0	138.2 ± 3.6	138.4 ± 5.3	0.592
K (mEq/L); mean ± SD	3.7 ± 0.3	3.7 ± 0.6	3.7 ± 0.7	0.998
Cl (mEq/L); mean ± SD	102.3 ± 7.4	100.3 ± 4.0	99.3 ± 7.6	0.89
Blood sugar (mg/dL); median [range]	26 [12–46]	80 [57–109]	84.5 [62–159]	<0.05
White blood cells (/μL) mean ± SD;	6067.5 ± 2880.3	4503 ± 1749.3	5213.3 ± 2799.2	0.591
Hemoglobin (g/dL); mean ± SD	12.1 ± 4.3	12.1 ± 3.9	12.8 ± 1.7	0.706
Platelet count (/μL); mean ± SD	10.4 ± 2.1	24.9 ± 7.9	25.3 ± 8.7	<0.05

AST, aspartate aminotransferase; BMI, body mass index; BUN, blood urea nitrogen; SD, standard deviation.

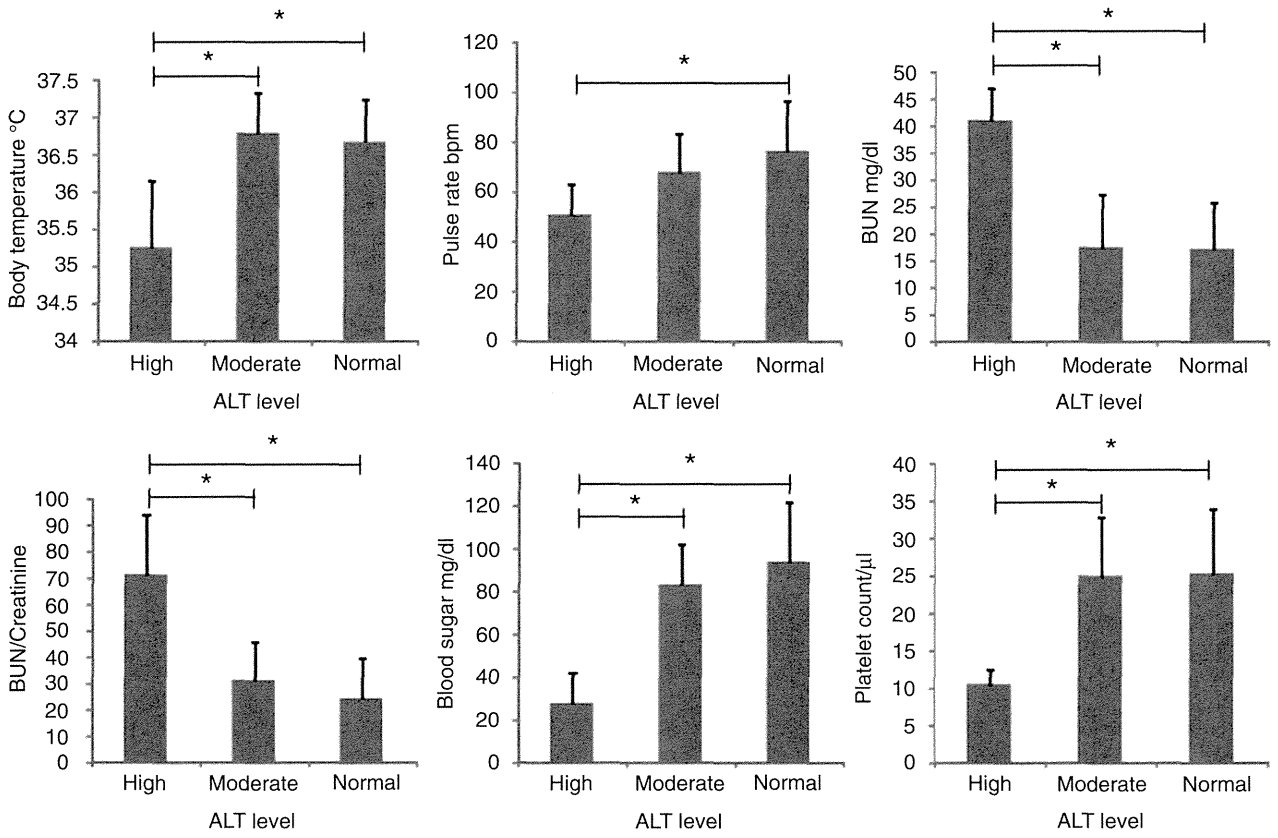

Figure 1 Statistically significant clinical parameters (body mass index [BMI], pulse rate, blood urea nitrogen [BUN], BUN/creatinine ratio, blood sugar, platelets count) among the three groups divided according to the severity of liver injury. Multiple comparisons (post hoc test) were performed with Tukey–Kramer and Steel–Dwass test. $^*P < 0.05$.

significantly lower in the high ALT group than in the normal ALT ($P < 0.05$) and moderate ALT ($P < 0.05$) groups. Pulse rate in the high ALT group was significantly decreased than in the normal ALT group ($P < 0.05$), but the difference between the high ALT and moderate ALT groups was not significant.

Risk factors related to elevated ALT levels in patients with AN

Among the six parameters (body temperature, pulse rate, BUN, BUN/creatinine, BS, platelet count) initially demonstrating significant differences among the three groups, risk factors relating to elevated ALT levels were examined. BUN/creatinine and BS were significantly associated with the incidence of elevated ALT by univariate analyses (Table 3). In further analysis with multiple logistic regression, there was not a significant association between the six parameters (body temperature, pulse rate, BUN, BUN/creatinine, BS, platelet count). However, there was a trend with BUN/creatinine (odds ratio [OR] = 1.051; 95% confidence interval [CI]; 0.999–1.105, $P = 0.054$) and BS (OR = 0.967; 95% CI; 0.933–1.002, $P = 0.066$ (Table 3).

DISCUSSION

WE FOUND THAT AN patients with highly elevated ALT had a significantly high BUN level and BUN/creatinine ratio, and a low body temperature, low blood sugar level, and low platelet count. Moreover, BUN/creatinine and BS had trends associated with the incidence of elevated ALT by multivariate analyses.

Clinical parameters in patients with AN demonstrating liver injury have been reported previously, especially the relationship between elevation of serum liver enzyme levels and low BMI.[6,7] However, in the present study, we found no significant correlation of serum liver

Table 3 Multiple logistic regression analysis related to elevated alanine aminotransferase (ALT) levels in anorexia nervosa (AN) patients

	Univariate		Multivariate	
	OR (95% CI)	*P*-value	OR (95% CI)	*P*-value
BUN/Creatinine (ratio)	1.051 (1.008–1.096)	0.019	1.051 (0.999–1.105)	0.054
Blood sugar (mg/dL)	0.962 (0.930–0.995)	0.025	0.967 (0.933–1.002)	0.066
Body temperature (°C)	0.509 (0.192–1.347)	0.174		
Pulse rates (bpm)	0.958 (0.916–1.002)	0.061		
BUN (mg/dL)	1.064 (0.997–1.135)	0.062		
Platelet count (/μL)	0.939 (0.866–1.019)	0.131		

Stepwise method was used to select the variables in multiple logistic regression analysis.
BUN, blood urea nitrogen; CI, confidence interval; OR, odds ratio.

enzyme levels with BMI. We speculate that this may have been attributable to the inclusion criteria we used for our AN patients. The present study recruited only AN patients who required hospitalization, so our study patients tended to have lower BMI values than outpatient studies, thus possibly masking any statistically significant differences.

Among several clinical parameters, we found that the serum BUN level and BUN/creatinine ratio were significantly high in the high ALT group. We speculate that this phenomenon could have been attributable to the presence of severe dehydration in this group, where a high BUN level and a high BUN/creatinine ratio (so-called "hypoxic hepatitis") were also observed. This is in accord with the fact that even patients with severe liver injury usually recover after conservative treatment such as drip infusion or bed rest, as seen in cases of hypoxic hepatitis due to circulatory failure occasionally encountered in various clinical settings.

We also observed that the high ALT group had significantly lower values of pulse rate. It seems paradoxical that AN patients with severe liver injury often have bradycardia despite the presence of severe dehydration. We speculate that this phenomenon may be due to the fact that patients with AN usually have hypertonic parasympathetic nervous conditions and hypotonic sympathetic nervous conditions, which lead to failure to respond to the stimulation of the sympathetic nervous system resulting from dehydration.[8] Also, among our AN patients in the high ALT group, hypoglycemia (median value as low as 26 mg/dL) was observed in four, and this led to consciousness disturbance in two. Up to now, there have been no convincing explanations for the hypoglycemia and liver injury associated with AN, although hypoglycemia could affect the systemic circulation, in turn influencing the hepatic circulation and resulting in liver injury. In fact, it has been reported that patients with hypoxic hepatitis are often complicated by hypoglycemia.[9]

In patients with AN, various complications known as "refeeding syndrome"can occur after initiation of food intake or hyperalimentation on admission and hypoglycemia is one of its symptoms.[10] Although some reports have described the presence of liver injury during hypoglycemia in refeeding syndrome,[11,12] its precise mechanism remains unknown.

Our present findings suggested a close relationship of dehydration in the pathogenesis of elevated liver enzyme in AN, with features clinically reminiscent of hypoxic hepatitis. However, we were not able to exclude the opposite possibility that high BUN and BUN/creatinine ratio could be caused by elevated ALTs. Unfortunately this is the limitation of this retrospective study. Our study was also limited in that it did not evaluate liver pathology. Hepatic histological findings in AN with liver insufficiency include centrilobular lesions with fibrosis or atrophy, hepatocytes swelling, glycogen depletion, and ceroid pigmentation.[13] Since almost all patients with AN are young females, who often have accompanying mood disorder and/or obsessive-compulsive disorder,[14] and liver injury rapidly improves after hospitalization,[15] invasive procedures such as liver biopsy are rarely performed at an early stage after admission when patients are psychiatrically unstable. Accordingly, future studies will need to evaluate liver histology or use an appropriate animal model.

In conclusion, the present study has demonstrated that AN patients with severe liver injury have significantly increased in the serum BUN level and BUN/creatinine ratio. This could account for failure of the

hepatic circulation due to severe dehydration based on malnutrition, being a potentially important factor in the development of severe liver injury in AN patients, mimicking hypoxic hepatitis. These factors offer an interesting insight into the pathogenesis of AN.

ACKNOWLEDGMENT

WE THANK MEMBERS of the Department of Psychiatry, Yamagata University Faculty of Medicine for their support and encouragement in this research.

REFERENCES

1 Kuboki T, Nomura S, Ide M, Suematsu H, Araki S. Epidemiological data on anorexia nervosa in Japan. *Psychiatry Res* 1996; **62**: 11–16.
2 Fong HF, DiVasta AD, DiFabio D, Ringelheim J, Jonas MM, Gordon CM. Prevalence and predictors of abnormal liver enzymes in young women with anorexia nervosa. *J Pediatr* 2008; **153**: 247–53.
3 De Caprio C, Alfano A, Senatore I, Zarrella L, Pasanisi F, Contaldo F. Severe acute liver damage in anorexia nervosa: two case reports. *Nutrition* 2006; **22**: 572–5.
4 Furuta S, Ozawa Y, Maejima K *et al.* Anorexia nervosa with severe liver dysfunction and subsequent critical complications. *Intern Med* 1999; **38**: 575–9.
5 Dowman J, Arulraj R, Chesner I. Recurrent acute hepatic dysfunction in severe anorexia nervosa. *Int J Eat Disord* 2010; **43**: 770–2.
6 Tsukamoto M, Tanaka A, Arai M *et al.* Hepatocellular injuries observed in patients with an eating disorder prior to nutritional treatment. *Intern Med* 2008; **47**: 1447–50.
7 Ozawa Y, Shimizu T, Shishiba Y. Elevation of serum aminotransferase as a sign of multiorgan-disorders in severely emaciated anorexia nervosa. *Intern Med* 1998; **37**: 32–9.
8 Petretta M, Bonaduce D, Scalfi L *et al.* Heart rate variability as a measure of autonomic nervous system function in anorexia nervosa. *Clin Cardiol* 1997; **20**: 219–24.
9 Fuhrmann V, Kneidinger N, Herkner H *et al.* Hypoxic hepatitis: underlying conditions and risk factors for mortality in critically ill patients. *Intensive Care Med* 2009; **35**: 1397–405.
10 Crook MA, Hally V, Panteli JV. The importance of the refeeding syndrome. *Nutrition* 2001; **17**: 632–7.
11 Sakurai-Chin C, Ito N, Taguchi M, Miyakawa M, Takeshita A, Takeuchi Y. Hypoglycemic coma in a patient with anorexia nervosa coincident with acute exacerbation of liver injury induced by oral intake of nutrients. *Intern Med* 2010; **49**: 1553–6.
12 Narayanan V, Gaudiani JL, Harris RH, Mehler PS. Liver function test abnormalities in anorexia nervosa-cause or effect. *Int J Eat Disord* 2010; **43**: 378–81.
13 Rautou P-E, Cazals-Hatem D, Mareau R *et al.* Acute liver cell damage in patients with anorexia nervosa: a possible role of starvation-induced hepatocyte autophagy. *Gastroenterology* 2008; **135**: 840–8.
14 Salbach-Andrae H, Lenz K, Simmendinger N, Klinkowski N, Lehmkuhl U, Pfeiffer E. Psychiatric comorbidities among female adolescents with anorexia nervosa. *Child Psychiatry Hum Dev* 2008; **39**: 261–72.
15 Giordano F, Arnone S, Santeusanio F, Pampanelli S. Brief elevation of hepatic enzymes due to liver ischemia in anorexia nervosa. *Eat Weight Disord* 2010; **15**: E294–7.

MCB
Journals.ASM.org

Nrf2 Enhances Cholangiocyte Expansion in Pten-Deficient Livers

Keiko Taguchi,[a,b] Ikuo Hirano,[b] Tohru Itoh,[c] Minoru Tanaka,[c] Atsushi Miyajima,[c] Akira Suzuki,[d] Hozumi Motohashi,[a] Masayuki Yamamoto[b]

Department of Gene Expression Regulation, Institute of Development, Aging and Cancer, Tohoku University, Sendai, Japan[a]; Department of Medical Biochemistry, Tohoku University Graduate School of Medicine, Sendai, Japan[b]; Laboratory of Cell Growth and Differentiation, Institute of Molecular and Cellular Biosciences, The University of Tokyo, Tokyo, Japan[c]; Division of Cancer Genetics, Department of Molecular Genetics, Medical Institute of Bioregulation, Kyushu University, Fukuoka, Japan[d]

Keap1-Nrf2 system plays a central role in the stress response. While Keap1 ubiquitinates Nrf2 for degradation under unstressed conditions, this Keap1 activity is abrogated in response to oxidative or electrophilic stresses, leading to Nrf2 stabilization and coordinated activation of cytoprotective genes. We recently found that nuclear accumulation of Nrf2 is significantly increased by simultaneous deletion of Pten and Keap1, resulting in the stronger activation of Nrf2 target genes. To clarify the impact of the cross talk between the Keap1-Nrf2 and Pten–phosphatidylinositide 3-kinase–Akt pathways on the liver pathophysiology, in this study we have conducted closer analysis of liver-specific *Pten*::*Keap1* double-mutant mice (Pten::Keap1-Alb mice). The Pten::Keap1-Alb mice were lethal by 1 month after birth and displayed severe hepatomegaly with abnormal expansion of ductal structures comprising cholangiocytes in a Nrf2-dependent manner. Long-term observation of Pten::Keap1-Alb::Nrf2$^{+/-}$ mice revealed that the Nrf2-heterozygous mice survived beyond 1 month but developed polycystic liver fibrosis by 6 months. Gsk3 directing the Keap1-independent degradation of Nrf2 was heavily phosphorylated and consequently inactivated by the double deletion of *Pten* and *Keap1* genes. Thus, liver-specific disruption of *Keap1* and *Pten* augments Nrf2 activity through inactivation of Keap1-dependent and -independent degradation of Nrf2 and establishes the Nrf2-dependent molecular network promoting the hepatomegaly and cholangiocyte expansion.

The Keap1-Nrf2 system is a critical defense mechanism against oxidative and electrophilic stresses (1). Nrf2 (nuclear factor erythroid 2-related factor 2) is a potent transcriptional activator that binds to antioxidant/electrophile-responsive elements (ARE/EpRE) with small Maf (2), leading to the upregulation of cytoprotective genes encoding antioxidant proteins, xenobiotic-detoxifying enzymes, and drug transporters. Keap1 (Kelch-like ECH-associated protein 1) is a cullin 3 (Cul3)-based E3 ubiquitin ligase adaptor that mediates the ubiquitination of Nrf2 in the cytoplasm, promoting the proteasomal degradation of Nrf2 under unstressed conditions. When cells are exposed to oxidative or electrophilic stresses, the cysteine residues of Keap1 are modified, resulting in the attenuation of Nrf2 ubiquitination. The Nrf2 that escapes Keap1-mediated degradation translocates into the nucleus and activates cytoprotective genes, conferring resistance to these stresses (3).

Recent studies have revealed that Nrf2 augments the metabolic reprogramming of cells in the presence of active proliferative signals, particularly the phosphatidylinositide 3-kinase (PI3K)–Akt pathway, through the activation of metabolic genes, resulting in the acceleration of cell proliferation (4, 5). Indeed, in various human cancer cells, Nrf2 is constitutively stabilized through genetic and/or epigenetic factors, promoting the proliferation of these cells (6–8). A similar association between cell proliferation signals and Nrf2 has been observed in *Keap1*-null mice, which exhibit the constitutive stabilization/activation of Nrf2 throughout the body. In *Keap1*-null mice, the cells of certain lineages are more proliferative than those of wild-type mice in an Nrf2-dependent manner. Basal layer keratinocytes in the upper digestive tract grow rapidly and cause obstructive thickening under conditions of defective Keap1 function (9–11). Immature megakaryocytes cultured from *Keap1*-null fetal livers also show rapid proliferation (12). These observations suggested that Nrf2 is a facultative or context-dependent accelerator of proliferation that does not inherently provoke cell cycle progression but requires proliferative signals to promote cell proliferation (13, 14). However, the molecular mechanisms and pathophysiological consequences of the expansion of Nrf2 function through active proliferative signals remain to be clarified.

Pten (phosphatase and tensin homolog deleted from chromosome 10) is a well-known tumor suppressor gene that counteracts the PI3K-protein kinase B (PKB)-Akt pathway. The functional loss of *Pten* increases Akt phosphorylation, which promotes cell growth, proliferation, and survival through the modulation of protein synthesis and metabolism (15). *PTEN* mutations and deficiencies are often detected in many types of human cancers (16). Approximately 40% of cases of hepatocellular carcinomas show a decrease or an absence of PTEN expression (17). Liver-specific *Pten* knockout mice serve as an animal model of liver carcinogenesis associated with nonalcoholic fatty liver disease (18, 19). These mice spontaneously develop hepatocellular carcinomas and, with less frequency, cholangiocellular carcinomas after they reach 1 year of age. We observed that Pten deficiency significantly augments Nrf2 accumulation in the nucleus (4). Considering that this observation reveals a molecular mechanism linking Nrf2 activation and cell proliferation signals (4), we initiated a study addressing the cross talk between the Keap1-Nrf2 system and the Pten-PI3K-Akt pathway.

To clarify the functional interactions of these pathways in the

Received 18 October 2013 Returned for modification 3 November 2013
Accepted 18 December 2013
Published ahead of print 30 December 2013
Address correspondence to Hozumi Motohashi, hozumim@idac.tohoku.ac.jp, or Masayuki Yamamoto, masiyamamoto@med.tohoku.ac.jp.

doi:10.1128/MCB.01384-13

liver, we generated *Pten*$^{flox/flox}$::*Keap1*$^{flox/flox}$::*Albumin*-Cre (Pten::Keap1-Alb) mice. *Pten*$^{flox/flox}$::*Albumin*-Cre (Pten-Alb) mice exhibit steatosis that progresses into tumorigenesis (18), whereas *Keap1*$^{flox/flox}$::*Albumin*-Cre (Keap1-Alb) mice do not exhibit apparent liver damage or dysfunction (11). Although Pten-Alb and Keap1-Alb mice survived longer, we found that the Pten::Keap1-Alb mice were lethal by 1 month after birth. Surprisingly, the Pten::Keap1-Alb mice displayed severe hepatomegaly, pathological liver enlargement by more than three times compared with normal average liver size, with abnormal expansion of the ductal structures comprising cholangiocytes. In contrast, Pten::Keap1-Alb::Nrf2$^{+/-}$ mice survived beyond 1 month, but these mice developed severe polycystic liver fibrosis, with the increased proliferation of cholangiocytes. These phenotypes were not observed in Pten::Keap1-Alb::Nrf2$^{-/-}$ mice, indicating the Nrf2 dependency of the phenotypes. The forced activation of Nrf2 in Pten-deficient livers results in consequences with respect to liver pathology that are completely different from those of single Pten deficiency in mice. Notably, we observed that the expansion of Nrf2 function in Pten and Keap1 double-knockout mice is established by the simultaneous inactivation of two distinct Nrf2 degradation pathways. Thus, the liver-specific disruption of *Keap1* and *Pten* establishes a new Nrf2-dependent molecular network, promoting proliferation of hepatocytes and cholangiocytes and skewing cell lineage development toward cholangiocytes.

MATERIALS AND METHODS

Mice. *Pten*$^{flox/flox}$, *Keap1*$^{flox/flox}$, and *Nrf2*$^{-/-}$ mice were previously described (18, 20, 21). The *Albumin*-Cre transgenic mouse was purchased from The Jackson Laboratory (Bar Harbor, ME) (22). These crosses generated *Pten*$^{flox/flox}$ (control), *Pten*$^{flox/flox}$::*Albumin*-Cre (Pten-Alb), *Keap1*$^{flox/flox}$::*Albumin*-Cre (Keap1-Alb), *Pten*$^{flox/flox}$::*Keap1*$^{flox/flox}$::*Albumin*-Cre (Pten::Keap1-Alb), *Pten*$^{flox/flox}$::*Keap1*$^{flox/flox}$::*Albumin*-Cre::*Nrf2*$^{-/-}$ (Pten::Keap1-Alb::Nrf2$^{-/-}$), and *Pten*$^{flox/flox}$::*Keap1*$^{flox/flox}$::*Albumin*-Cre::*Nrf2*$^{+/-}$ (Pten::Keap1-Alb::Nrf2$^{+/-}$) mice. A Rosa-26 reporter (R26R) mouse (23) was used for the β-galactosidase assay. DNA was obtained from each mouse and genotyped using PCR. The mice were provided water and rodent chow *ad libitum*. All mice were maintained under specific-pathogen-free conditions and treated according to the regulations of The Standards for Human Care and Use of Laboratory Animals of Tohoku University and Guidelines for Proper Conduct of Animal Experiments of the Ministry of Education, Culture, Sports, Science, and Technology of Japan. The plasma was analyzed using Fuji Dri-Chem 7000 (Fujifilm Corp., Tokyo, Japan) to detect alanine transferase (ALT), aspartate transferase (AST), lactate dehydrogenase (LDH), total cholesterol (TCHO), total bilirubin (TBIL), direct bilirubin (DBIL), albumin (ALB), uric acid (UA), and blood urea nitrogen (BUN).

Immunoblot analysis. The tissues were homogenized in 9 volumes of 0.25 M sucrose, and the 10% homogenate was filtered through a 100-μm-pore-size membrane. The nuclear fraction was prepared using Dignam's method with some modifications (24). The cells were lysed in SDS sample buffer (50 mM Tris-HCl [pH 6.8], 10% glycerol, 2% SDS). The protein concentration was determined using a bicinchoninic acid (BCA) protein assay kit (Pierce Biotechnology, Rockford, IL), with bovine serum albumin as the standard. The samples were resolved using SDS-polyacrylamide gel electrophoresis and transferred onto a polyvinylidene difluoride membrane (Millipore, Billerica, MA). The following antibodies were used: anti-Nrf2 (25), anti-Keap1 (26), anti-Pten (catalog no. 9559; Cell Signaling Technology Inc., Danvers, MA), anti-LaminB (catalog no. sc-6217; Santa Cruz Biotechnology Inc., Dallas, TX), anti-Nqo1 (catalog no. ab2346; Abcam PLC, Cambridge, United Kingdom), anti-pAkt (T308) (catalog no. 9275; Cell Signaling Technology), anti-pAkt (S473) (catalog no. 9271; Cell Signaling Technology), anti-Akt (catalog no. 9272; Cell Signaling Technology), anti-phosphorylated glycogen synthase kinase (pGSK)3α/β (Ser21/9; GSK3α preferred, catalog no. 9327; Cell Signaling Technology), anti-GSK3α/β (catalog no. 5676; Cell Signaling Technology), and anti-α-tubulin (catalog no. T9026; Sigma-Aldrich).

TABLE 1 Primers and probes used in the RT-qPCR[a]

Primer	Oligonucleotide sequence	Reference
G6pc-F	5′-CGACTCGCTATCTCCAAGTGA-3′	48
G6pc-R	5′-GTTGAACCAGTCTCCGACCA-3′	
Alb-F	5′-GACGTGTGTTGCCGATGAGT-3′	
Alb-R	5′-GTTTTCACGGAGGTTTGGAATG-3′	
Krt19-F	5′-CGGTGGAAGTTTTAGTGGGA-3′	49
Krt19-R	5′-AGTAGGAGGCGAGACGATCA-3′	
Trop2-F	5′-CTGACCTAGACTCCGAGCTG-3′	50
Trop2-R	5′-CGGCCCATGAACAGTGACTC-3′	
Ggt1-F	5′-AACAGGAGCAAGAGTGGGAC-3′	51
Ggt1-R	5′-GGTGGCCTCCATTTATTGC-3′	
Gclc-F	5′-ATCTGCAAAGGCGGCAAC-3′	11
Gclc-R	5′-ACTCCTCTGCAGCTGGCTC-3′	
Gclc-P	5′-FAM-ACGGGTGCAGCAAGGCCCA-TAMRA-3′	
Gpx2-F	5′-TGTCAGAACGAGGAGATCCTG-3′	11
Gpx2-R	5′-GACTAAAGGTGGGCTGGTACC-3′	
Gpx2-P	5′-FAM-CAATACCCTCAAGTATGTCCGACCTG-TAMRA-3′	
Hes1-F	5′-TCAACACGACACCGGACAAAC-3′	11
Hes1-R	5′-ATGCCGGGAGCTATCTTTCTT-3′	
Jag1-F	5′-ATGCAGAACGTGAATGGAGAG-3′	
Jag1-R	5′-GCGGGACTGATACTCCTTGAG-3′	
rRNA-F	5′-CGGCTACCACATCCAAGGAA-3′	11
rRNA-R	5′-GCTGGAATTACCGCGGCT-3′	
rRNA-P	5′-FAM-TGCTGGCACCAGACTTGCCCTC-TAMRA-3′	

[a] FAM, 6-carboxyfluorescein; RT-qPCR, reverse transcription-quantitative PCR; TAMRA, 6-carboxytetramethylrhodamine.

Histological analysis. The livers were fixed in Mildform 10N (Wako Pure Chemical Industries, Ltd., Osaka, Japan) and embedded in paraffin for staining with hematoxylin and eosin (HE) and Masson trichrome. For immunohistochemical staining, the livers were processed as previously described (27), using anti-cytokeratin 19 (anti-CK19) antibody (28). The positive reactivity was visualized through sequential incubation with EnVision^{+} Dual Link System-horseradish peroxidase (HRP) (Dako) and diaminobenzidine (DAB) staining. Hematoxylin was used for nuclear counterstaining. Using a Zamboni-fixed frozen section, immunohistochemical staining against anti-Trop2 (catalog no. AF1122; R&D Systems) and anti-EpCAM (catalog no. 118201; BioLegend) antibodies was performed according to the methods described in a previous report (29) using an LSM 510 Meta confocal microscope equipped with ZEN2008 software (Carl Zeiss, Oberkochen, Germany). X-Gal (5-bromo-4-chloro-3-indolyl-β-D-galactopyranoside) staining was performed according to the method described in a previous report (30) with slight modifications.

RNA purification and reverse transcription-quantitative PCR (RT-qPCR). Total RNA was isolated from the liver using Isogen (Nippon Gene) and transcribed into cDNA using SuperScript III reverse transcriptase (Life Technologies Corp., Carlsbad, CA). qPCR analysis was performed using the Applied Biosystems 7300 PCR system and qPCR Mas-

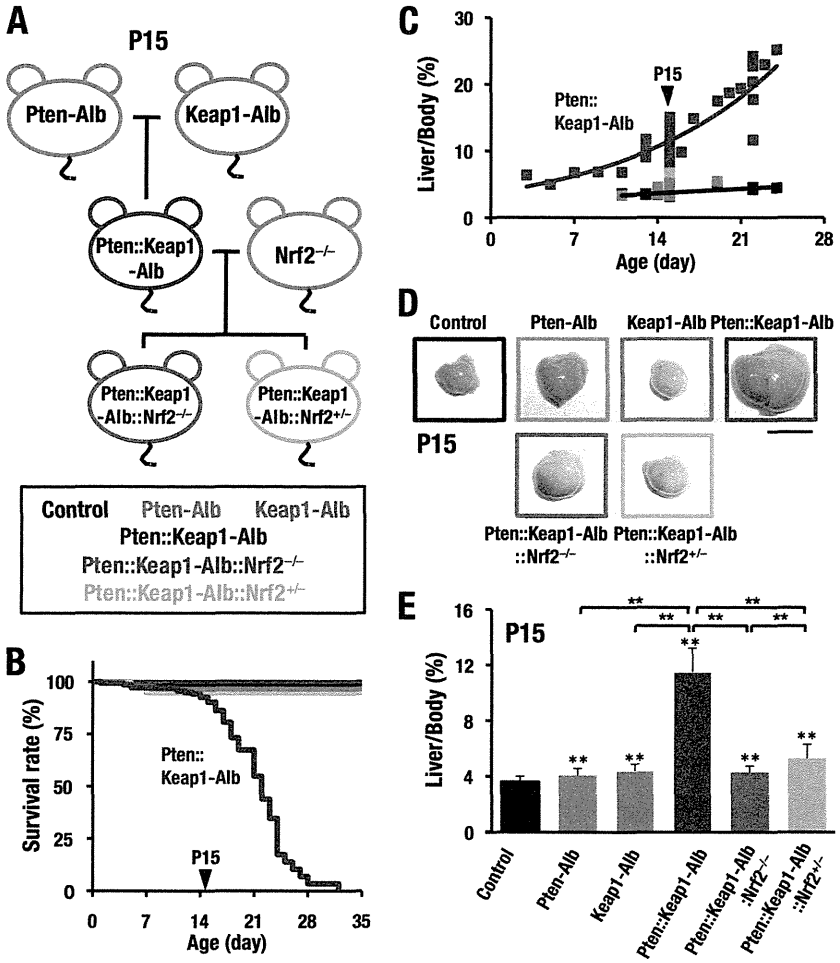

FIG 1 Lethality and hepatomegaly in Pten::Keap1-Alb mice. (A) Mating strategy for the generation of compound mutant mice of *Pten*, *Keap1*, and *Nrf2* genes. A detailed examination was conducted on postnatal day 15 (P15). (B) Survival rates up to P35 ($n \geq 50$). (C) Changes in liver-to-body-weight ratios to P28 ($n = 11$ to 53). (D) Representative macroscopic observation of the livers at P15. The scale bar corresponds to 1 cm. (E) Liver-to-body-weight ratios at P15 ($n = 12$ to 44). **, $P < 0.01$.

termix Plus (Eurogentec) or Power SYBR green PCR master mix (ABI). The data were normalized to rRNA expression. The primers and probes used for amplification of cDNAs are described in Table 1.

Microarray analysis. Total RNA from the liver was labeled with Cy3. The samples were hybridized to whole-mouse-genome Oligo DNA Microarray kit ver2.0 (Agilent Technologies, Inc., Santa Clara, CA) according to the manufacturer's protocol. Arrays were scanned using a G2539A microarray scanner system (Agilent), and the resulting data were analyzed using GeneSpring GX software (Agilent).

Statistical analysis. The average values were calculated, and the error bars indicate standard deviations. The differences were analyzed using Student's *t* test. $P < 0.05$ was considered statistically significant.

Microarray data accession number. The microarray data obtained in this study have been submitted to the Gene Expression Omnibus (GEO) database (http://www.ncbi.nlm.nih.gov/geo/) and assigned GEO accession number GSE50575.

RESULTS

Simultaneous disruption of *Pten* and *Keap1* in the liver results in hepatomegaly and lethality. We initially hypothesized that the constitutive stabilization of Nrf2 exacerbates liver carcinogenesis caused by Pten disruption. To address this hypothesis, we conducted a detailed analysis of *Pten* and *Keap1* double-mutant mice, in which both genes were deleted through Cre recombinase expression under conditions the regulation of the *Albumin* gene (Pten::Keap1-Alb mice). We compared the Pten::Keap1-Alb mice with $Pten^{flox/flox}$ (control) mice and *Pten* single-mutant mice or *Keap1* single-mutant mice (Pten-Alb or Keap1-Alb mice, respectively). The mating strategy for the generation of *Pten* and *Keap1* compound mutant mice is shown in Fig. 1A. The results for the control, Pten-Alb, Keap1-Alb, and Pten::Keap1-Alb mice are depicted in black, red, light blue, and dark blue, respectively, in this figure and in the remaining figures shown in this study.

We observed that Pten::Keap1-Alb mice were born with Mendelian inheritance, and the appearance of the newborns was normal. The body weight gain of double-knockout mice was indistinguishable from that of control or individual single-knockout mice (data not shown). The body weights at postnatal day 15 (P15) were comparable in all genotypes examined (data not shown). Surprisingly, the Pten::Keap1-Alb mice started dying after the second week, and all the mice of this genotype died within 35 days after birth (Fig. 1B). We observed slight abdominal swelling of the double-mutant mice at 2 weeks of age (data not shown). Therefore, we examined the livers of the Pten::Keap1-Alb mice at P15. Figure 1C shows the liver-to-body-weight ratio of the Pten::Keap1-Alb mice (dark

blue squares) in comparison with control (black), Pten-Alb (red), and Keap1-Alb (light blue) mice. We observed that the livers of the double-knockout mice became gradually larger after birth and were markedly enlarged by P15 (Fig. 1C and D). While the magnitude of hepatomegaly was markedly significant in the Pten::Keap1-Alb double-knockout mice, the single knockouts of *Pten* or *Keap1* (Pten-Alb or Keap1-Alb mice) showed slight but significant hepatomegaly (Fig. 1E).

A closer examination of the dissected livers revealed the enlargement of the liver of the double-knockout mice, but no whitish appearance or signs of liver steatosis, characteristic phenotypes in mature Pten-Alb mice, were observed (18) (Fig. 1D). The livers of Pten single-knockout mice were also normal in appearance at P15. Notably, the livers of the Pten::Keap1-Alb mice were yellowish, indicating the development of jaundice (Fig. 1D). In addition, the plasma and urine of these mice were also yellowish (data not shown). These results demonstrate that the double deletion of *Pten* and *Keap1* in the liver results in juvenile death and abnormal hepatomegaly.

Hepatomegaly and lethality observed in *Pten* and *Keap1* double-knockout mice are Nrf2 dependent. Because one of the most prominent targets of Keap1-mediated ubiquitination is Nrf2, we hypothesized that Nrf2 plays a role in the hepatomegaly and lethality of double-mutant mice. To examine this hypothesis, we generated Pten::Keap1-Alb::Nrf2$^{-/-}$ and Pten::Keap1-Alb::Nrf2$^{+/-}$ mice by crossing Pten::Keap1-Alb mice and *Nrf2*-null mice, which do not show any apparent abnormalities in livers. The mating strategy for the generation of the compound mutant for *Pten*, *Keap1*, and *Nrf2* genes in mice is also shown in Fig. 1A. The results for the Pten::Keap1-Alb::Nrf2$^{-/-}$ and Pten::Keap1-Alb::Nrf2$^{+/-}$ mice are depicted in dark green and light green, respectively, in this figure and in the remaining figures shown in this study.

Notably, the lethality of Pten::Keap1-Alb mice was clearly abrogated in the *Nrf2*-null background (Fig. 1B). As a result of deleting *Nrf2*, the liver enlargement in the double-mutant mice was reduced to levels similar to those observed in the single-knockout mouse (Fig. 1C to E). Even the single-allele deletion of *Nrf2* was effective for the alleviation of the lethality and liver phenotypes. Thus, these results demonstrate that the Pten::Keap1-Alb mice display hepatomegaly and eventual lethality that is Nrf2 dependent.

***Pten* and *Keap1* double-mutant mice display cholangiocyte expansion and liver dysfunction.** Because Pten::Keap1-Alb mice died at approximately 2 weeks of age, we selected P15 as a time point for the pathological analyses. The histological examination of Pten::Keap1-Alb mouse livers using Masson trichrome staining revealed a marked increase of tubular structures, primarily bile ducts, and connective tissue in the region of the hepatic triad, which is the anatomically close association of hepatic artery, vein, and bile duct. Masson trichrome staining enabled clearer detection of collagen fibers and tubular structures than hematoxylin-eosin staining. The features observed in Pten::Keap1-Alb mouse livers were completely absent in control, Pten-Alb, and Keap1-Alb mice (Fig. 2Aa, b, e, and f and data not shown). We confirmed the increase of cholangiocytes using CK19 staining (28). CK19-positive staining abnormally accumulated in the double-mutant livers (Fig. 2Aj). There were no histological signs of steatosis in the livers of Pten::Keap1-Alb mice.

We also examined biochemical parameters in the blood of these double-mutant mice (Fig. 2B, left four bars). Levels of indicators of liver damage, alanine transferase (ALT), aspartate transferase (AST), and lactate dehydrogenase (LDH), were all higher in Pten::Keap1-Alb mice than in control and single-mutant mice. Total cholesterol (TCHO) levels and the direct bilirubin/total bilirubin (DBIL/TBIL) ratio were both increased in Pten::Keap1-Alb mice, suggesting the presence of bile congestion in the livers of the Pten::Keap1-Alb mice. We also examined albumin (ALB) as a marker of liver function and observed that the level of this protein was maintained within a normal range in the plasma of Pten::Keap1-Alb mice, although the plasma ALB level was slightly reduced in Keap1-Alb single-knockout mice. The biochemical examination together with the histological analysis indicates that Pten::Keap1-Alb mice display abnormal cholangiocyte expansion concomitant with cholestasis and liver damage.

Abnormal expansion of cholangiocytes and liver damage in *Pten* and *Keap1* double-mutant mice are Nrf2 dependent. To determine whether the abnormal expansion of cholangiocytes and the liver damage were provoked by the increase in Nrf2, we examined the livers of Pten::Keap1-Alb::Nrf2$^{-/-}$ triple-mutant mice. The histological examination revealed the disappearance of abnormal bile duct formation and connective tissues (Fig. 2Ac and g). The accumulation of CK19-positive cholangiocytes in double-mutant mice was abrogated in Pten::Keap1-Alb::Nrf2$^{-/-}$ mice (Fig. 2Ak). Elevated levels of ALT, AST, LDH, and TCHO and the DBIL/TBIL ratio in Pten::Keap1-Alb mice were all reduced in Pten::Keap1-Alb::Nrf2$^{-/-}$ mice to control levels (Fig. 2B, dark green bars). The ALB level in Pten::Keap1-Alb::Nrf2$^{-/-}$ mice was not different from that in mice of the other genotypes (Fig. 2B, dark green bars). We concluded that constitutively stabilized Nrf2 mediates cholangiocyte expansion and liver damage in the absence of Pten.

To further delineate the precise contribution of Nrf2, we examined the effect of the single-allele disruption of Nrf2 in the Pten::Keap1-Alb background. In the heterozygote livers, the CK19-positive cholangiocytes did not increase substantially (Fig. 2Ad, h, and l), and the biochemical parameters were within the normal range (Fig. 2B, light green bars). However, further examination of the livers of Pten::Keap1-Alb::Nrf2$^{+/-}$ mice revealed mild fibrosis spreading from the hepatic triad (Fig. 2Ad and h). Thus, we propose that chronic exposure to mild Nrf2 signals under conditions of Pten deficiency might provoke unexpected pathologies in heterozygote livers.

***Pten* and *Keap1* double-mutant cells contribute to cholangiocyte expansion.** To determine whether the cholangiocyte expansion in Pten::Keap1-Alb mouse livers were primarily derived from *Pten* and *Keap1* double-mutant cells, we performed a lineage-tracing analysis using Rosa-26 reporter mice, in which the floxed β-galactosidase reporter gene is integrated into the Rosa-26 locus. It has been reported that the majority of hepatocytes and cholangiocytes can be monitored by crossing the Rosa-26 reporter mice with *Albumin*-Cre mice (19). This double-lineage labeling by β-galactosidase in this monitoring line of mice demonstrates that the albumin promoter is functional in hepatoblasts, a common progenitor of hepatocytes and cholangiocytes (31). We observed that, in Pten::Keap1-Alb mice crossed with Rosa-26 reporter mice, not only hepatocytes but also all expanded cholangiocytes were positively stained for the β-galactosidase activity (Fig. 3B and D). The LacZ-positive tubular structures near the portal vein were CK19-positive cholangiocytes (Fig. 3F and H). Both hepatocytes